IMPACT OF FE (III) ON THE PERFORMACE OF VISCOELASTIC SURFACTANT-BASED ACIDS

A Thesis

by

YI SHU

Submitted to the Office of Graduate Studies of
Texas A&M University
in partial fulfillment of the requirements for the degree of

MASTER OF SCIENCE

Chair of Committee,	Hisham A. Nasr-El-Din
Committee Members,	Jerome J. Schubert
	Mahmoud El-Halwagi
Head of Department,	Daniel Hill

August 2013

Major Subject: Petroleum Engineering

ABSTRACT

Viscoelastic surfactant (VES)-based acid systems have been used successfully in matrix and acid fracturing treatments. However, the existence of Fe (III) as a contaminant in such systems may lead to many problems, due to interactions between VES and Fe (III). Such interactions can reduce the effectiveness of VES-based acid systems and potentially lead to formation damage.

In this study, two VES's were selected and reaction mechanisms between VES and Fe (III) were studied. Rheological properties of these two surfactants were examined with various concentrations of Fe (III). An energy dispersive X-ray spectroscopy (EDS) was used to identify precipitates from reaction products. Inductively coupled plasma (ICP) was applied to measure iron concentrations, and the two-phase titration method was used to determine VES concentrations in all liquid phases of the sample. The effect of several chelating agents on the reaction of VES with Fe (III) was also examined.

Experimental results indicate that the apparent viscosity of live VES-based acids (20 wt% HCl, 4 vol% VES) increased from 3 to 131 cp at a shear rate of 100 s^{-1} at room temperature when the Fe (III) concentration increased from 0 to 2,300 ppm, and started to decrease at higher Fe (III) concentrations. This is because of the electrostatic interactions between negative charged $[FeCl_4]^-$ groups and positive charged amine groups in VES in live acids. Both surfactants interacted with Fe (III), and precipitates, which are complexes containing iron and VES, were noted at 5,000 ppm and higher concentrations of Fe (III).

On the other hand, adding a chelating agent [1:1 mole ratio to Fe (III)] helped in reducing the apparent viscosity of the sample, which means that the chelating agent reacted with Fe (III) and reduced interactions between VES and Fe (III). At the same time, coreflood setup was also used. With a chelating agent, Fe (III) was recovered in 98%, which was much higher than that without any chelating agent (46%). These results provided a clue of the protection effect of a chelating agent on VES-based acid in Fe (III) containing environment. Adding a suitable chelating agent can minimize the impact of Fe (III) on VES-based acids.

ACKNOWLEDGEMENTS

I would like to thank my advisor, Dr. Hisham A. Nasr-El-Din, and my committee members, Dr. Jerome J. Shubert and Dr. Mahmoud El-Halwagi, for their guidance and support throughout the course of this research.

Thanks also go to my friends and colleagues and the department faculty and staff for making my time at Texas A&M University a great experience.

Finally, thanks to my mother and father for their encouragement and to my wife for her patience and love.

NOMENCLATURE

P	Pressure, psi
t	Time, minutes
Q	Flow rate, cm^3/s
A	Cross-sectional area to flow, cm^2
k	Permeability, md
μ	Fluid viscosity, cP
γ	Shear rate, s^{-1}
K	Reaction constant
f	Activity coefficient

TABLE OF CONTENTS

Page

Page

LIST OF FIGURES

Page

Page

Page

Page

LIST OF TABLES

Page

CHAPTER I

INTRODUCTION AND LITERATURE REVIEW

1.1. Carbonate Matrix Acidizing

Formation damage may be caused by many reasons, such as clay migration, drilling-mud invasion, and inorganic scaling. Usually, matrix acidizing is one of the most effective methods to solve this problem. By dissolving the materials plugging the pore spaces or creating new pathways (wormholes), a successful treatment of matrix acidizing will reduce skin factor and thus improve well productivity.

In carbonate reservoirs, hydrochloric acid (HCl) is the first and the easiest method used in acidizing. This was first done by the Ohio Oil Company in 1895, and such method was first recorded in 1896 (Williams et al. 1979). Untill now, HCl was still the method generally conducted in carbonate reservoirs. However, some organic acids, such as acetic or formic acid, which are less corrosive, are used, when the temperature is high and the corrosion of HCl causes a problem.

When HCl is used to the carbonate reservoir, the carbonate rocks, mainly calcite and dolomite, can react and dissolve in HCl rapidly. The reaction equations are described as follows (**Eq. 1** and **Eq. 2**):

$$CaCO_3 \text{ (calcite)} + 2\ HCl \rightarrow CaCl_2 + CO_2 + H_2O \quad (1)$$

$$CaMg(CO_3)_2 \text{ (dolomite)} + 4\ HCl \rightarrow CaCl_2 + MgCl_2 + 2\ CO_2 + 2\ H_2O \quad (2)$$

The reaction between calcite and HCl is much faster than the one between dolomite and HCl, and the reaction rate is determined by the delivery speed of the acid

to the surface of the rock. At the same time, generation of irregularly shaped channels inside of rocks can increase production better than simply face washing away rocks (Economides et al. 1994).

However, directly using HCl could lead to severe corrosion to the wellhead and the tubing. In 1931, Dr. John Grebe of the Dow Chemical Company found arsenic has a corrosion inhibition capacity of HCl on metal. In 1932, arsenic was used along with 500 gallons of HCl that was pumped into a dead limestone well by the Michigan-based Pure Oil Company. This treatment lead to the first successful commercial acidizing service: the production of this dead limestone well increased from 0 to 16 bbl/day (Williams et al. 1979). In the following years, different companies developed a wide range of acid additives to enhance the effectiveness of HCl treatment. Such additives include corrosion inhibitors, surfactants, pH buffers, friction reducers, etc..

Proper diversion is very important during the acid treatment to achieve the maximum benefit. Without any diversion, acid would enter the region with the highest permeability. Thus, the damaged zone would hardly be treated.

Several diverting agents and methods were developed in recent years. For example, fluids can be directed to the target zone via drillpipes or coiled-tubing tools with mechanical packers. Bridging agents such as benzoic acid particles can help to create filter cake in wormholes in carbonate reservoirs. Such filter cake can block the acid flow and force it to divert into the zone with lower permeability.

If a diverting agent is applied, some basic and important principles that have to be followed:

1. The diverting agent can effectively divert acid fluids.
2. The diverting agent should have a very low solubility in the carrying fluids.
3. The diverting agent should be easily and efficiently removed.

When the viscosity of the acid increases during an acid treatment, the acid spending rate decreases to lead to a deeper acid penetration (Deysarkar et al. 1984). Based on this, high-viscosity fluids were developed and have been applied during matrix acidizing and acid-fracturing treatments.

Polymers and viscoelastic surfactants (VES) are the most common additives applied to increase the viscosity of an acid fluid. Uncross-linked polymers are not as effective as the acid soluble polymers or the cross-linked polymers which were introduced in the mid-1970s. These polymers can increase the viscosity of the injection fluid to improve the performance of HCl (Pabley et al. 1982; Yeager and Shuchart 1997; Metcalf et al. 2000). To apply cross-linked polymers in in-situ gelled acids, what usually contains acid, polymer, crosslinker, breaker, buffer, and other possible additives. As pH increases above a specific value, the polymer will be crossliked to form a gel. Generally, in-situ gelled acids are good to use. However, under certain conditions, some problems may be noted. For example, in tight carbonate reservoirs at high temperatures, or in sour environments, the crosslinker [Fe (III)] may precipitate (Lynn and Nasr-El-Din 2001; Nasr-El-Din et al. 2002).

To overcome these problems, surfactant-based acids were developed. The most common viscoelastic surfactants include amineoxide surfactants and betaine (carboxybetaine and sulfobetaine) surfactants (Fu and Chang. 2005). The general sketch

of a VES molecule is shown in **Fig. 1** (Al-Nakhi et al. 2008). It contains a partly hydrophilic head with oxygen and nitrogen atoms along with carbon and hydrogen atoms. At the same time, it has a tail with a long carbon-hydrogen chain which is hydrophobic.

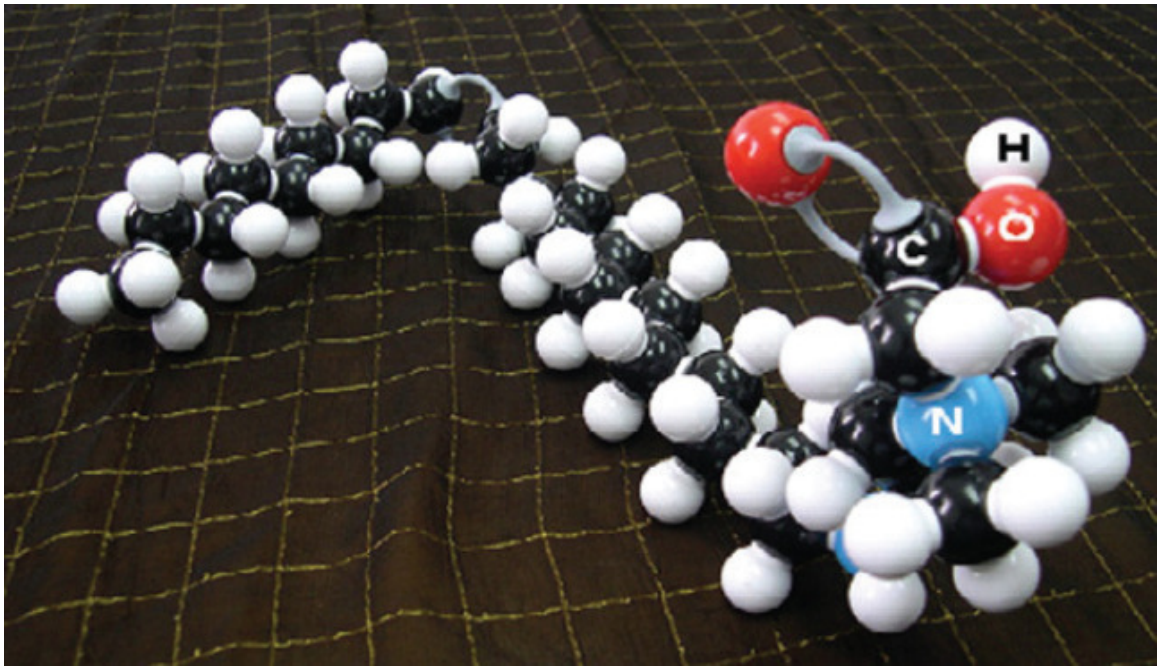

Fig. 1—General molecular sketch of a VES molecule.

Typically, VES is applied with HCl. Such VES-based acids have been used over the last few years in matrix and acid fracturing treatments. Once the acid reacts with the carbonate formation, the pH increases above 2 and the concentration of calcium and magnesium ions increases. These VES's can form long, rod-shaped micelles. These micelles can entangle and form a 3D structure as shown in **Fig. 2**. This formation of micelles would lead to an increase in the apparent viscosity of the solution to provide a

better acid diversion and deeper acid penetration in the matrix acid treatment. (Chang et al. 1998; Card et al. 1999).

The formed gelled-acid can be broken down by a reverse mechanism of formation such gels in different ways:

1. Injecting water to reduce the concentration of metal ions and/or VES;

2. Preflushing with mutual solvents to revert micelle shape from rods to sphere;

3. Applying internal breakers if necessary. Internal breakers can be mixed with VES fluid at surface and go wherever the fluids goes; ensure the VES fluid breaks; and break the VES fluid into an easily producible fluid (Crews and Huang 2007).

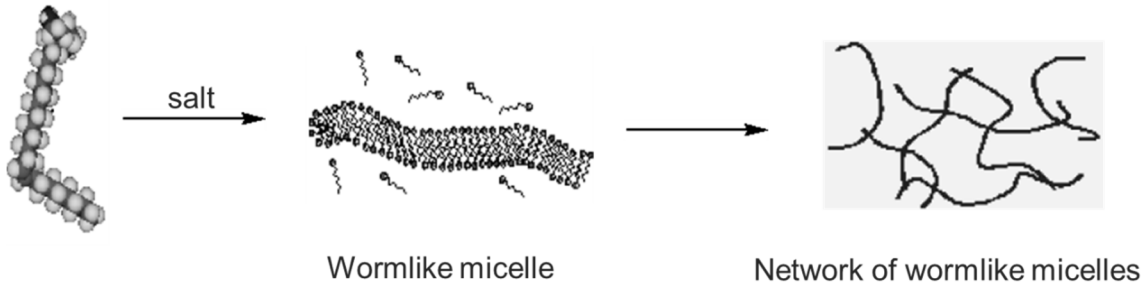

Fig. 2—A schematic illustration of an entangled wormlike micelles network.

1.2. Iron Related Problems

Iron precipitation is one of the most serious problems during acid treatment. Both forms of iron, Fe (II) and Fe (III), could lead to formation damage under different conditions. In addition, the source of iron varies: the storage and mixing tanks, the tubulars and pipeline, and the iron minerals in the formation (Dill and Fredette 1983, Hall and Dill 1988).

Some iron compounds are soluble in live acids, however, they may still precipitate in spent acids. Fe (III) hydroxide starts to precipitate at a pH of about 1 and completes at a pH of about 2 at 25°C (Taylor et al. 1999).

Compared to Fe (III), Fe (II) is not a serious problem in sweet environment because it will not start to precipitate until the pH value of the solution is higher than 6.5 (Dill et al. 1983). However, Fe (II) can be easily oxidized by the oxygen dissolved in the solution to form Fe (III). Moreover, Fe (II) may also lead to formation damage. The free Fe (II) ion is a reactive iron material in the precipitation of iron sulfide with the existence of H_2S (Frenier et al. 2000). The reaction is showed as follows (**Eq. 3**):

$$Fe^{2+} + S^{2-} \rightarrow FeS\downarrow \quad (3)$$

Moreover, both Fe (II) and Fe (III) could promote sludging of certain asphaltic crude (Jacobs and Thorne 1986).

1.3. Impact of Fe (III) on VES-Based Acids

VES-based acids were used in hundreds of successful treatments. However, the results of one treatment were below expectations. Analysis of the live acid used indicates that this acid contains near 10,000 mg/l iron. Interaction between iron and VES is the most possible reason. Such interactions may reduce the effects of VES-based acid and may even lead to formation damage. While in the field, rust in storage and mixing tanks can be dissolved by acid and produce a mixture of Fe (III) and Fe (II). Fe (II) can be further oxidized to Fe (III) by the oxygen in the solution. As a result, the existence of Fe (III) cannot be avoided completely. According to Gougler et al. (1985), iron content at

the wellhead varies from 200 to 3,500 mg/l and the returning acid shows iron concentrations of 9,000 to 100,000 mg/l during cleanup treatments of new wells.

Since the Fe (III) is the most possible factor that can adversely affect the behavior and function of VES-based fluids, studies on such effects are necessary and important.

1.4. Application of Chelating Agents on Iron Control

Chelating agents are chemicals that form soluble, complex molecules with certain ion, inactivating the ions so that they cannot normally react with other elements or ions to produce precipitates or scale. By applying chelating agents, free metal ions in solution could be bound due to the formation of two or more separate coordinate bonds between the metal ion and the chelating agent. Several chelating agents are applied today. Ethylenediaminetetraacetic acid (EDTA), nitrilotriacetic acid (NTA), and citric acid (as shown in **Fig. 3**), etc. are the most used ones.

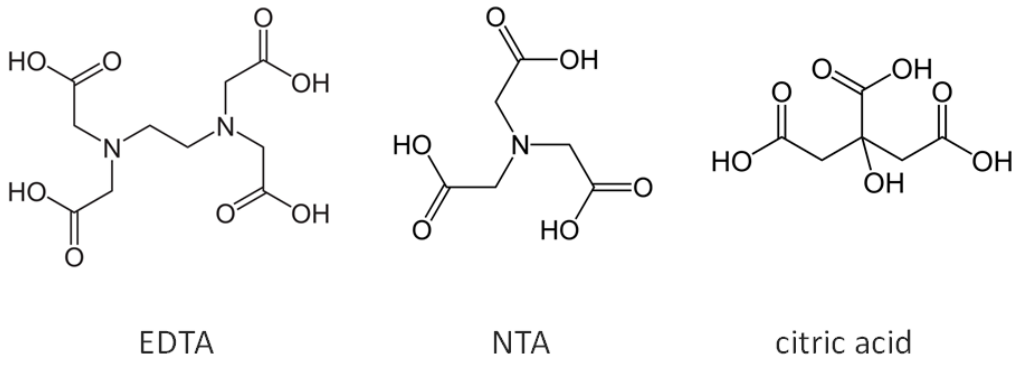

Fig. 3—Molecular structures of EDTA, NTA, and citric acid.

Fig. 4 shows a general bonding mechanism between a Fe (III) ion and the EDTA molecule. Similarly, a Ca (II) ion and the NTA molecule can also form a complex in the same way.

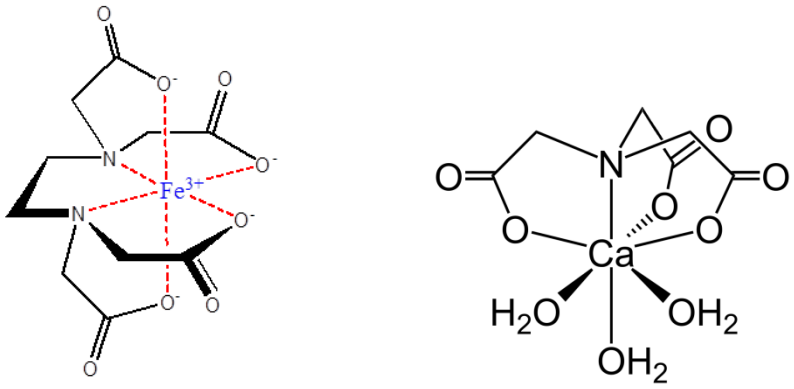

Fig. 4—Coordinative bonding mechanisms of EDTA-Fe (left) and NTA-Ca (right) complexes.

1.5. Research Objectives

Objectives of this research on the interaction between Fe (III) and VES are to:

1. Understand conditions under which Fe (III) has effects on VES-based acid systems.

2. Investigate the mechanism of the interaction between Fe (III) and VES.

3. Evaluate iron control agents (GLDA-NaH_3 and HEDTA-NaH_2) in VES-based acid systems.

CHAPTER II

EXPERIMENTAL STUDIES

2.1. Materials

Ferric chloride ($FeCl_3$) and concentrated hydrochloric (HCl) acid (37 wt%, American Chemical Society grade) were used as received. The concentration of HCl acid was determined by titration with a 1 mol/l sodium hydroxide (NaOH) solution.

The acid indicator solution of the two-phase titration was prepared by the methods introduced by Rosen et al. (1987), and details on the procedure to measure surfactant concentrations in live/spent acid was discussed by Yu et al. (2011).

The titrant (sodium dodecanesulfonate, > 99%) and the two main components of the indicator solution, dimidium bromide (95% HPLC) and acid blue (Patent Blue V C.I.) were used. Other materials included ethanol (CH_3CH_2OH, ACS/USP grade) and chloroform ($CHCl_3$, 100 wt%). All solutions were prepared using de-ionized (DI) water with a resistivity of 18.2 MΩ·cm at 25°C.

Corrosion inhibitors and viscoelastic surfactants are the oilfield chemicals that were used as received. The components of the corrosion inhibitor (CI-5) are listed in **Table 1**.

Table 1—Components of CI-5.

Name	CAS #	% by Weight
Ethoxylated fatty amines	Proprietary	37
Fatty amines	Proprietary	28
Progargyl alcohol	107-19-7	15
Acetic acid	64-19-7	5
Formaldehyde	50-00-0	6
Water	7732-18-5	9

In this study, the VES APA-TW, which is an amine oxide with a molecular weight of 382.62 g/mol, is named as VES-1 with a molecular structure shown in **Fig. 5**.

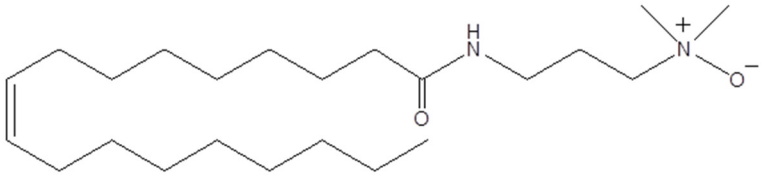

Fig. 5—Molecular structure of VES-1.

The general molecular formula of VES-2 is shown in **Fig. 6**.

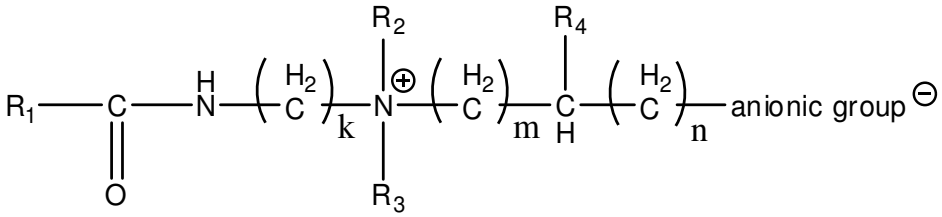

Fig. 6—General molecular formula of VES-2.

2.2. Equipment

A Fann Model 35 viscometer was used to measure the apparent viscosity of acid solutions. The concentration of iron (Fe) ions in solution was measured by Inductivity Coupled Plasma (ICP) analysis using the Optima 7000DV ICP-OES system and WinLab 32TM software. The elemental composition of selected precipitates from the samples was examined by Evex Mini Scanning Electron Microscope (SEM) with MSC-1000 Mini-Sputter Coater and Energy Dispersive X-ray Spectroscopy (EDS). The effect of chelating agents on VES-based acid systems were evaluated by the Fann Model 35 viscometer and a coreflood setup. The pH of the solutions was determined via Thermo scientific Orion Ross electrode.

2.3. Measurements

Rheology and viscosity measurements of all VES systems were made using a viscometer at room temperature and atmospheric pressure. The elemental analysis was carried out by ICP and EDS. And the concentration of VES was tested via a two-phase titration method that was introduced by Rosen et al. (1987). Details on the procedure to measure surfactant in live/spent acid were discussed by Yu et al. (2009).

The indicator solution of the two-phase titration experiment was prepared as follows (Rosen et al., 1987): 0.050 g dimidium bromide (**Fig. 7**) was dissolved in 10 cm^3 of hot $EtOH/H_2O$ (1:9 vol) solution using a 50 cm^3 beaker. In the second 50 cm^3 beaker, dissolve 0.050 g disuphine blue V (**Fig. 8**) was dissolved in 10 cm^3 hot $EtOH/H_2O$ (1:9 vol) solution. The content of the second beaker was transferred to the first one and

washed with 5 cm^3 hot EtOH/H_2O (1:9 vol) solution. The mixed solution was transferred into a brown bottle. 100 cm^3 de-ionized water, 25 cm^3 1mol/l H_2SO_4 solution, and 100 cm^3 de-ionized water were added subsequently while stirring.

The mechanism of the two-phase titration method is as follows (Yu et al., 2009): In a two-phase system of organic phase (chloroform) and aqueous phase, sample surfactant complexes with disulphine blue molecules in the aqueous phase displace into the organic phase, which has a blue color. After the addition of the titrant, sodium dodecanesulfonate (**Fig. 9**), to this two-phase system, the complex reacts with the titrant. So the blue color of the organic phase starts to fade. When the end point is reached, titrant molecules complex with ethidium bromide molecules in the aqueous phase and displace into the organic phase to make it reveal a purple color. At the end point, the complex of [dimidium bromide]$^+$[dodecanesulfonate]$^-$ turns the color of the organic phase into a light purple color.

Aqueous phase:

[surfactant] + H^+ + [disulphine blue V]$^-$ → [surfactant-H]$^+$[disulphine blue V]$^-$ (blue, to the orgaince phase)

Organic phase:

[surfactant-H]$^+$[disulphine blue V]$^-$ + [dodecanesulfonate]$^-$ (from the aqueous phase) → [surfactant-H]$^+$[dodecanesulfonate]$^-$ (colorless) + [disulphine blue V]$^-$ (to the aqueous phase)

At the end point:

[dimidium bromide] (aqueous phase) + [dodecanesulfonate]$^-$ (aqueous phase) → [dimidium dodecanesulfonate]$^-$ (light purple, to the organic phase) + Br^-

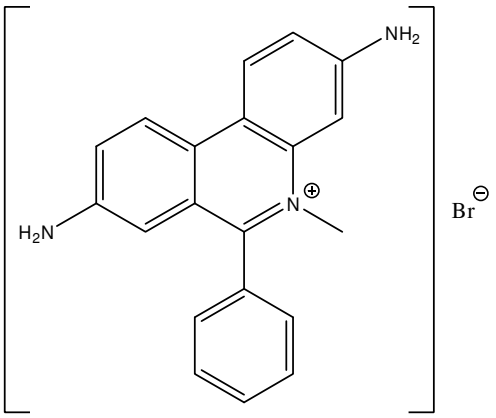

Fig. 7—Molecular structure of dimidium bromide.

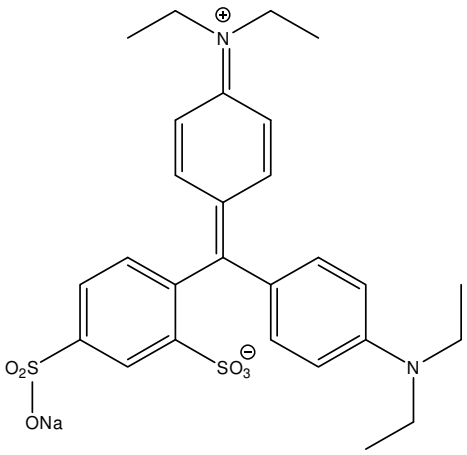

Fig. 8—Molecular structure of disulphine blue V (acid blue).

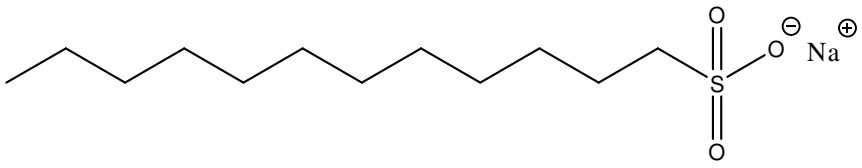

Fig. 9—Molecular structure of sodium dodecansulfonate.

2.4. Two-Phase Titration Procedures

Ethanol (10.00 ml) was added into the VES solution and de-ionized water was added until the total volume was 50.00 ml. A 10.00 ml sample solution was transferred to an Erlenmeyer flask with a glass stopper. Then, 10 ml of acid mixed indicator solution, 0.234 ml concentrated H_2SO_4, 15 ml chloroform, and 2.40 ml ethanol were added ordinally. The mixture was shaken and titrated by 1.000 mmol/l of dodecanesulfonate-water solution. The two-phase mixture was shaken vigorously after each addition of titrant. Stop adding titrant when the organic phase turned from blue to light purple and record the volume.

A calibration working curve was plotted and the sample data was fitted in this working curve to get the concentration of the VES in sample solution.

CHAPTER III

PROPERTY MEASUREMENTS OF VES-1-BASED ACIDS AND THE FE (III)-VES-1 REACTION MECHANISM

3.1. VES-1-Based Acids with 3 wt% HCl

The existence of Fe (III) may lead to formation damage in VES-based acids, especially when the concentration of Fe (III) is high. However, in some cases, even with a very high concentration of Fe (III) (10,000 ppm) in the VES-based acids, no precipitation or phase separation was observed. Also, the apparent viscosity of the acids did not change much with various concentrations of Fe (III) (Al-Nakhli et al. 2008). As a result, the study on the condition under which Fe (III) has effects on VES-based acid systems is very important.

First, the VES-1-based acids were prepared at a concentration of 3 wt% of HCl and transferred to sample tubes, as shown in **Fig. 10**. Different amount of $FeCl_3$ [the source of Fe (III)] was added to achieve the targeted Fe (III) concentrations. All samples contained 4 vol% VES, 3 wt% HCl, and various Fe (III) concentrations.

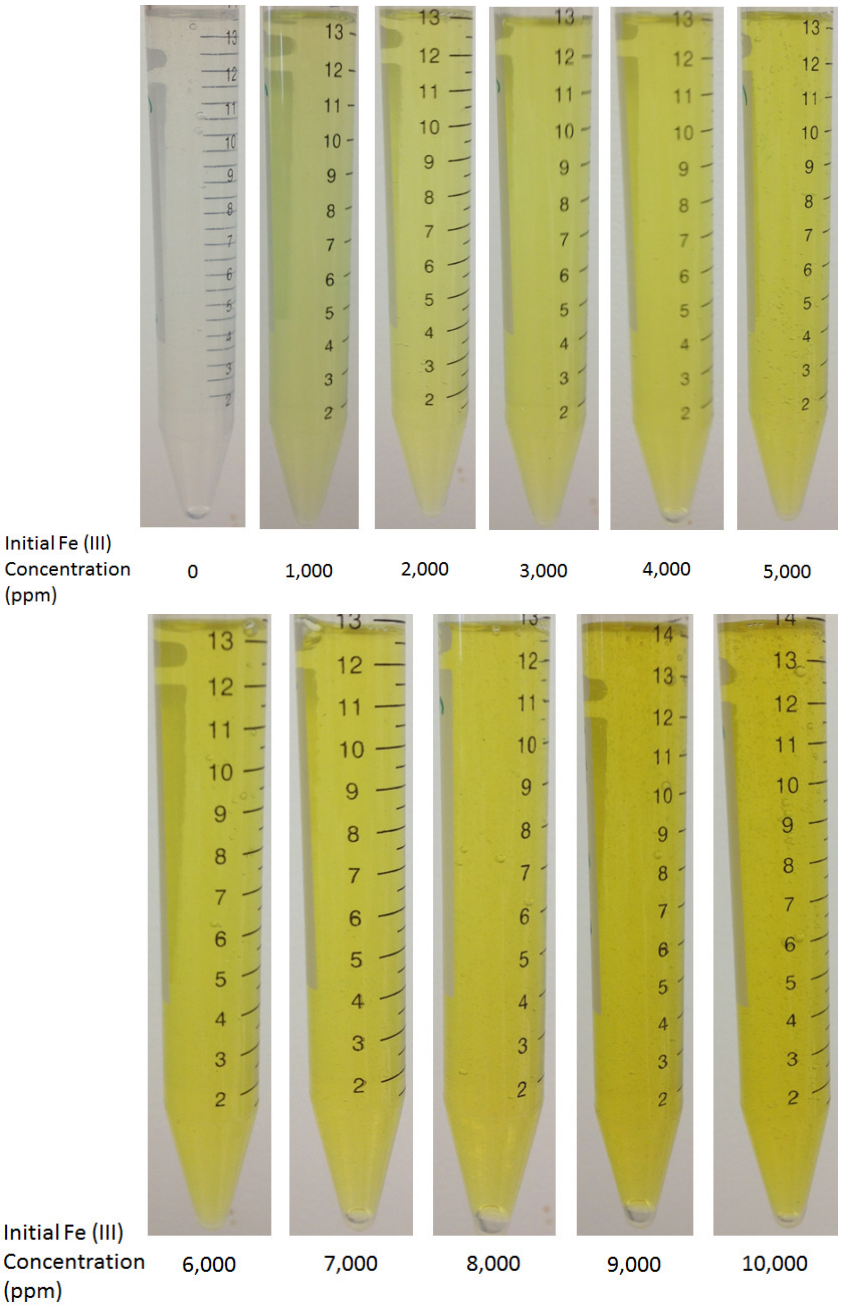

Fig. 10—Samples of VES-1-based acids: 4 vol% VES-1, 3 wt% HCl, and various concentrations of Fe (III). Freshly prepared at room temperature. The color of solutions turned to yellow, which became darker as the Fe (III) concentration increased.

As shown in **Fig. 10**, with the increase of Fe (III) concentrations, the sample color became a darker yellow. However, no phase separation or precipitation was observed. Then, the apparent viscosities of all samples at a shear rate of 100 s^{-1} were measured at room temperature and plotted in **Fig. 11**.

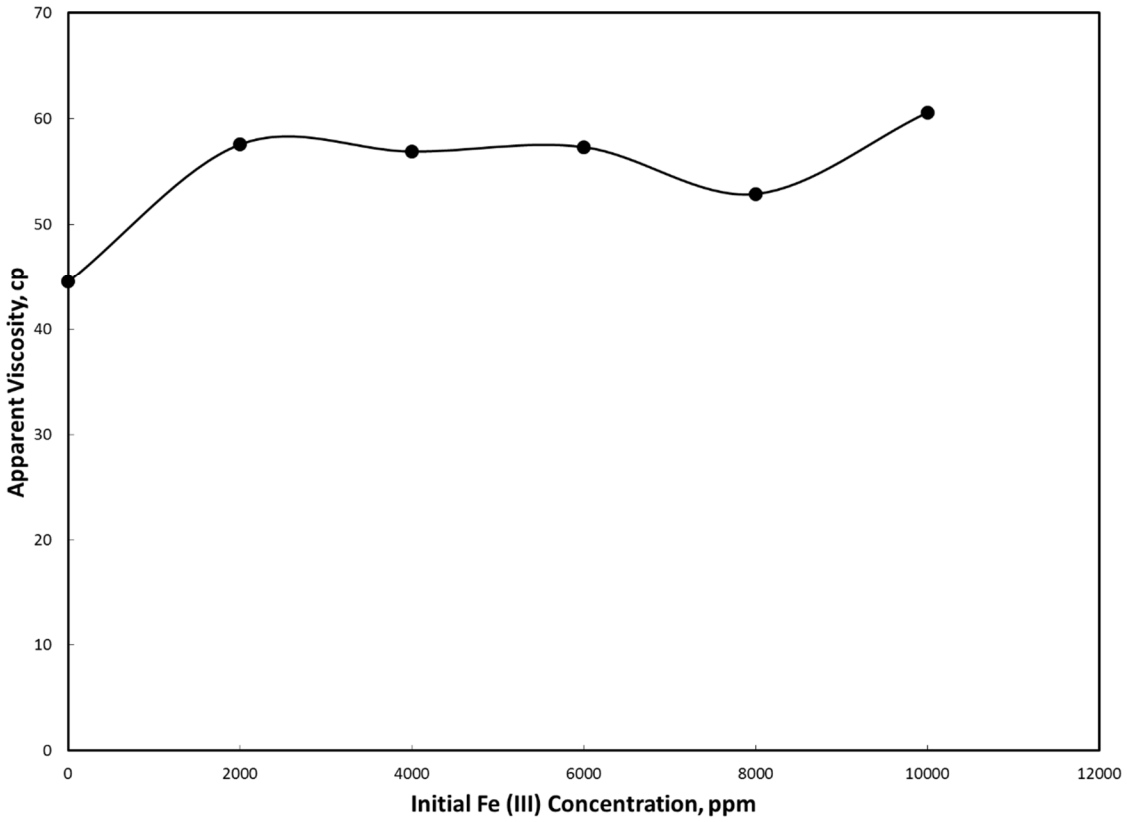

Fig. 11—Apparent viscosity of VES-1 solutions at different concentrations of Fe (III) at room temperature and at a shear rate of 100 s^{-1}. VES-1-based acids showed similar apparent viscosities at various Fe (III) concentrations when the HCl concentration was 3 wt%.

It is clear that the apparent viscosity of VES-1-based acid stayed around 50 to 60 cp and did not change much with the increase of Fe (III) concentrations.

Such results match previous work (Al-Nakhli et al. 2008): at an HCl concentration of 3 wt%, Fe (III) does not have much impact on the VES-based acid systems. However, severe formation damage was noticed during acidizing with VES-based acid at a higher HCl concentration. It is easy to come to the hypothesis that the HCl concentration plays an important role during this process.

Based on the above, the study here starts with the investigation of the interaction between Fe (III) and two different kinds of VES. Rheological properties of two VES's [APA-TW (VES-1) and ACAR-11016 (VES-2)] were tested with various concentrations of Fe (III). Methods of inductively coupled plasma (ICP), Energy Dispersive X-ray Spectroscopy (EDS), and two-phase titration were used to analyze the samples during the test. All sample solutions tested contain 20 wt% HCl and 4 vol% VES in DI water. $FeCl_3$ was added to the live acids to make samples containing various Fe (III) concentrations from 1,000 to 10,000 ppm (1,000 to 10,000 mg/l).

3.2. Samples Preparation: VES-1 with 20 wt% HCl

All samples contained 4 vol% VES-1, 20 wt% HCl, and various Fe (III) concentrations at a total volume of 40 cm^3.

1. A 50 cm^3 test tube was filled with weighted $FeCl_3$ powder, and a calculated volume of DI water was injected to make a homogenous solution.

2. HCl (37 wt%, 21.6 cm^3) was measured and transferred into the tube followed by addition of 1.6 cm^3 VES-1.

3. DI water was added until the total volume of the sample reached 40 cm^3.

4. All sample tubes were shaken violently to make sure all chemicals added were mixed well.

All samples were transferred into the same tubes and shown in **Fig. 12**:

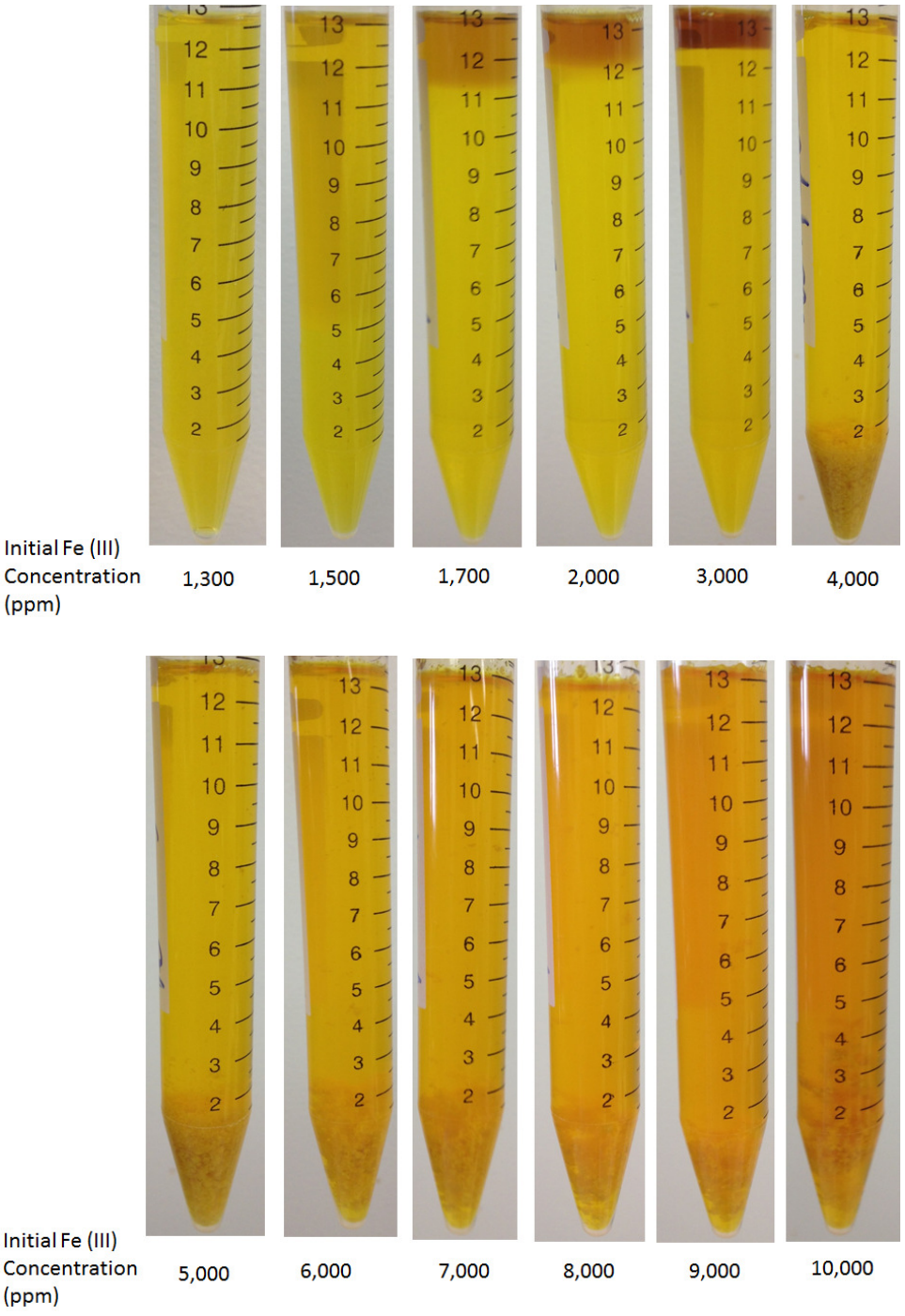

Fig. 12—Samples of VES-1-based acids: 4 vol% VES-1, 20 wt% HCl, and various concentrations of Fe (III). Freshly prepared at room temperature.

As shown in **Fig. 12**, when Fe (III) concentration was lower than 1,300 ppm, no phase separation or precipitation was observed in the VES-1-based acid. At a Fe (III) concentration of 1,500 ppm, phase separation was noticed. As shown in **Fig. 13**, the sample was enlarged to find the phase separation face easier, since the top phase was only a little darker yellow than the bottom phase.

Fig. 13—Phase separation face in the sample of VES-1-based acid with 1,500 ppm Fe (III) at a HCl concentration of 20 wt% at room temperature.

With higher Fe (III) concentrations (1,700 to 3,000 ppm), such phase separation became easier to be recognized because the color of the top phase had turned progressively darker. Simultaneously, when the Fe (III) concentration reached as high as 4,000 ppm, along with the phase separation, a brown precipitate was found at the same time. Such phenomenon was also noticed at the Fe (III) concentration of 5,000 ppm [as

shown in **Fig. 12** and **Fig. 14** (the enlarged top part of the sample)]. However, when the Fe (III) concentration was higher than 5,000 ppm (6,000 to 10,000 ppm, as shown in **Fig. 12**), only brown precipitates were obtained at the bottom and the color of the liquid portion would become progressively darker with increase in Fe (III) concentrations.

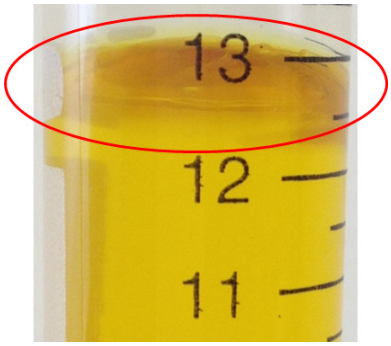

Fig. 14—Existence of phase separation in a sample of VES-1-based acid with 5,000 ppm Fe (III) at a HCl concentration of 20 wt% and at room temperature.

3.3. Apparent Viscosity Measurements

Fig. 15 shows the effects of different Fe (III) concentrations on the viscosity of a VES-1 acid system at room temperature and at the shear rate of 100 s^{-1}.

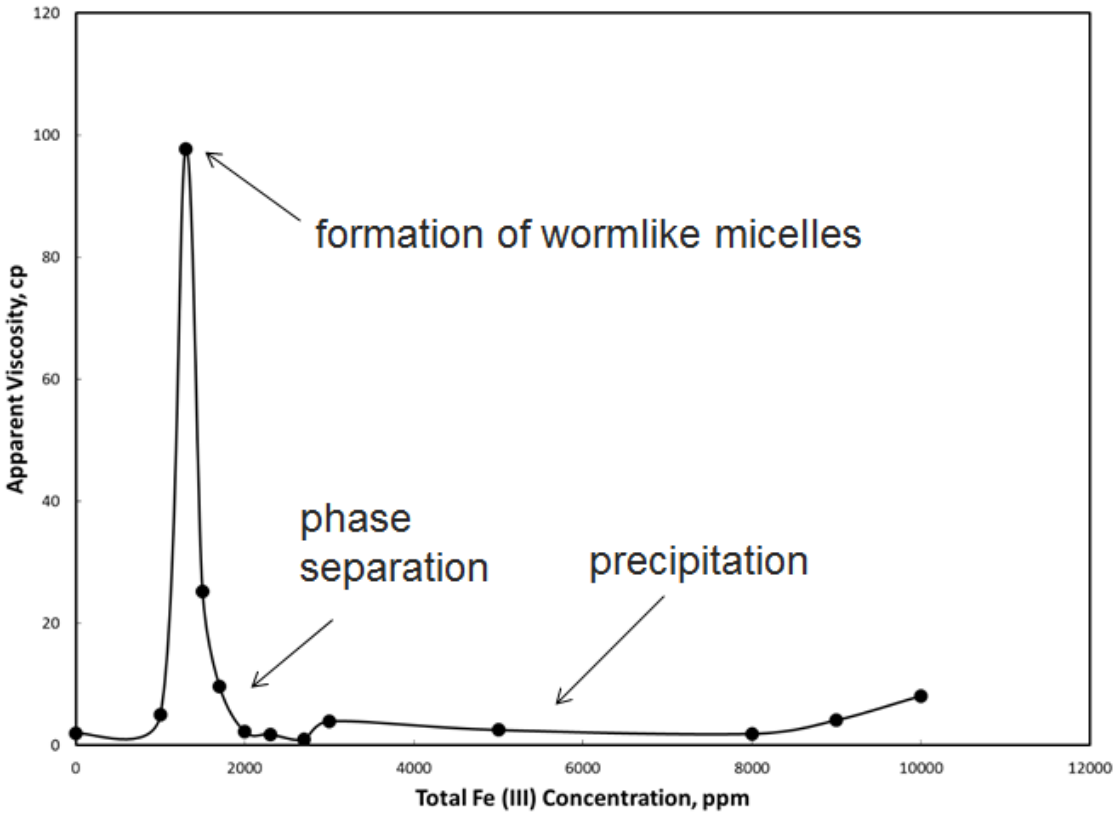

Fig. 15—Apparent viscosity of VES-1 solutions at different concentrations of Fe (III) at room temperature and at a shear rate of 100 s^{-1}. VES-1-based acids showed different apparent viscosities because of the various Fe (III) concentrations at a HCl concentration of 20 wt%.

The apparent viscosity of VES-1-based acid systems was very low (about 2 cp at room temperature and a shear rate of 100 s^{-1}). In **Fig. 15**, the apparent viscosity of VES-1-based acids increased at low Fe (III) concentrations and then reached the highest point (97.7 cp) at the Fe (III) concentration of 1,300 ppm. After this point, the sample apparent viscosity decreased at higher Fe (III) concentrations.

When comparing the apparent viscosity data to the direct observation of all VES-1 samples, the Fe (III) concentration was no more than 1,300 ppm, the solution was clear and more viscous than without Fe (III) to about 97.7 cp. When the Fe (III) concentration was in the range of 1,500 to 5,000 ppm, there was a phase separation and the apparent viscosity of the sample decreased back to around 2 cp. While the Fe (III) concentration is higher than 5,000 ppm, precipitates were observed, while the apparent viscosity of the sample remained at a very low level (less than 8 cp).

This observation implies the presence of interactions between Fe (III) and VES-1. Long rod-shape micelles are formed at a relatively low Fe (III) concentrations and VES-1 is reacted before it can reach the designed location during the treatment in the field. Also, in the environment with a high Fe (III) concentration (higher than 1,500 ppm), the phase separation or formation of precipitates may lead to possible formation damage.

3.4. Concentration Measurements: VES Concentrations

The concentrations of VES-1 in all samples were titrated via the two-phase titration method and the results were plotted in **Fig. 16**.

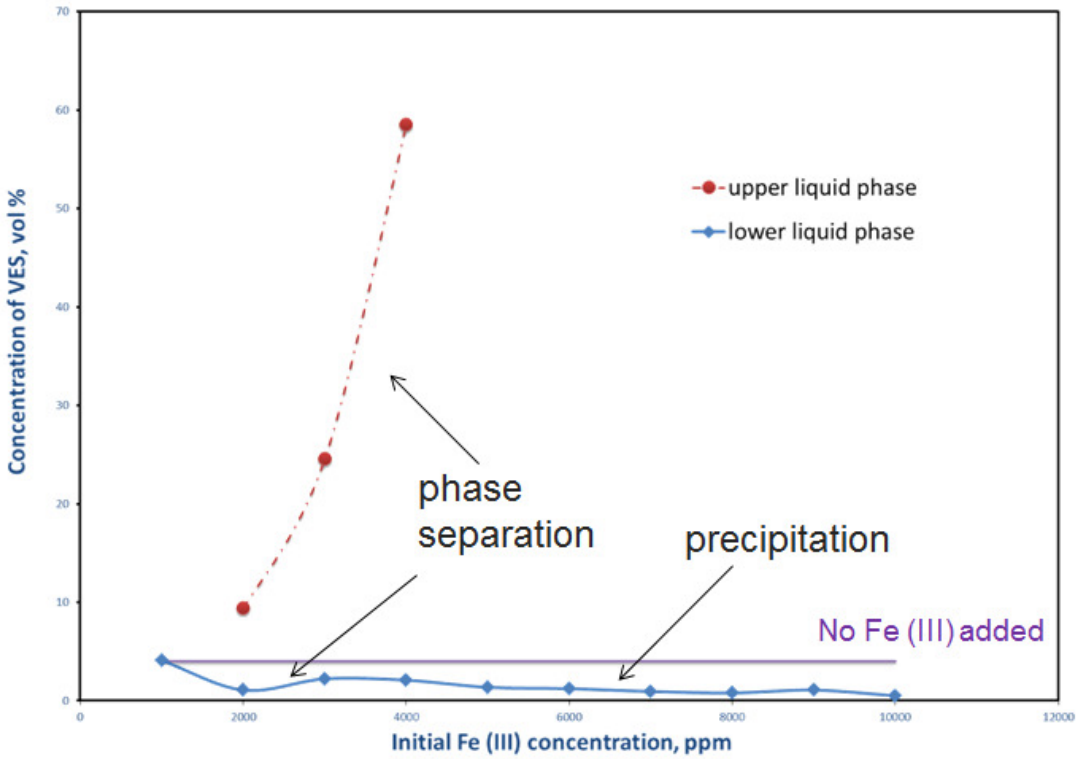

Fig. 16—Concentrations of VES-1 in the presence of various concentrations of Fe (III) at room temperature, freshly prepared.

As discussed above, there was a phase separation in samples containing 2,000, 3,000, and 4,000 ppm of Fe (III). So to these samples, the concentration of VES-1 of both phases was titrated. As shown above, when the Fe (III) concentration is as low as 1,000 ppm, the solution was still clear and the VES-1 concentration stayed at about 4 vol%. However, when the concentration of Fe (III) became higher, between 2,000 and 4,000 ppm, the phenomenon of phase separation was observed. In these three samples, the bottom phase was a light yellow in color while the upper phase was in brown. According to the results of the titration, the concentration in the bottom phase was

decreased to about 1-2 vol% and the the upper phase had a much higher VES-1 concentration: 10 vol% at 2,000 ppm of Fe (III), 24 vol% at 3,000 ppm of Fe (III), and 59 vol% at 4,000 ppm of Fe (III). It is obvious that the VES-1 reacted with Fe (III) and became concentrated in the upper phase. At the same time, the volume of upper phase became less. When the concentration of Fe (III) increased to 5,000 ppm and higher, instead of the phase separation, a dark brown precipitate was obtained. At the same time, the concentration of VES-1 in the solution decreased to as low as about 1 vol%. Such results have indicated that the VES-1 could be precipitated by Fe (III) and the concentration of VES-1 in solution would be greatly decreased when the VES-1 acid system was displaced in the environment with 5,000 ppm or higher Fe (III).

3.5. Concentration Measurements: Fe (III) Concentrations

The concentration of iron (Fe) ions in the solution was analyzed by an Inductivity Coupled Plasma (ICP) analysis using the Optima 7000DV ICP-OES system and WinLab 32TM software. Samples were diluted to make sure the concentration of iron ions was between 5 and 30 mg/l to fit the best measurement range. Then the iron concentrations in the original samples were calculated and plotted in **Fig. 17**.

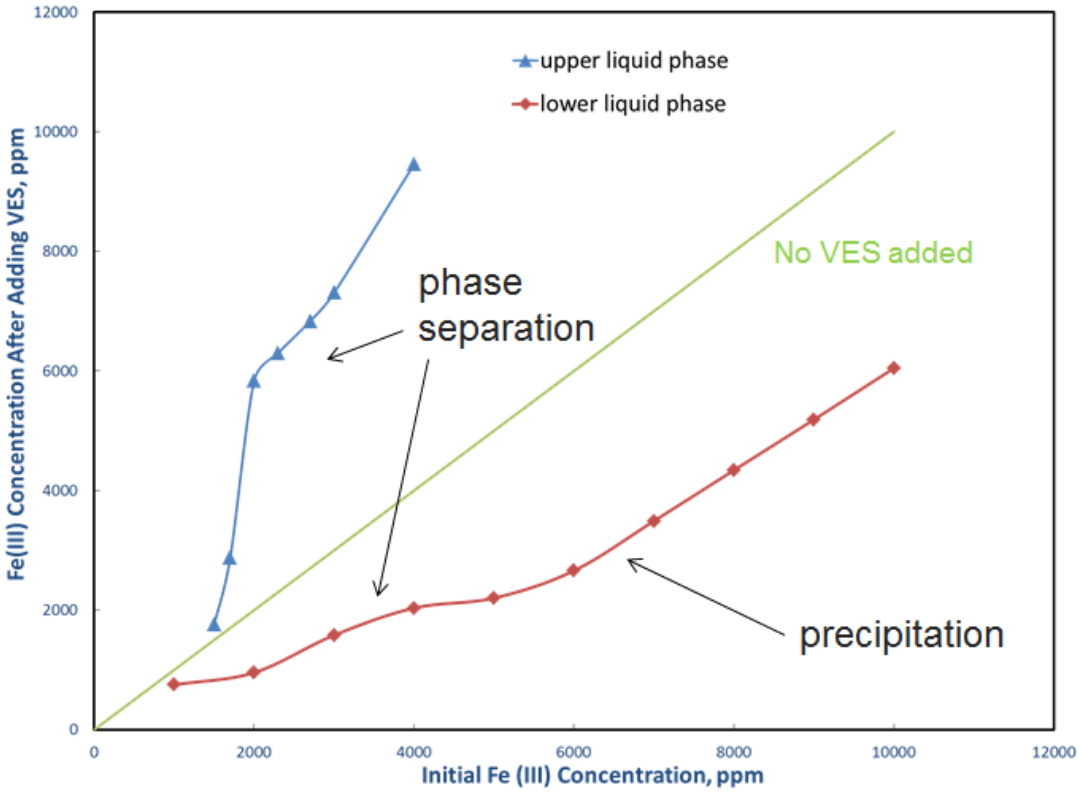

Fig. 17—Fe (III) concentrations in the liquid phases in all VES-1-based acid samples at room temperature.

Fig. 17 shows the concentration of Fe (III) in the solution of freshly prepared VES-1 acid samples. When the initial concentration of Fe (III) was 1,000 ppm, even though it was mixed with the VES-1 sample, the concentration of Fe (III) did not decrease much. However, when the initial concentration of Fe (III) became higher than 1,500 ppm, there was a phase separation. In the upper phase, Fe (III) concentration increased along with VES-1 concentrations (as shown in **Fig. 16**). When the initial concentration of Fe (III) was higher than 5,000 ppm, precipitates formed. At the same

time, as shown in the graph, the difference between initial Fe (III) concentration and the measured Fe (III) concentration became larger when the initial concentration is higher than 5,000 ppm. This means part of the Fe (III) remained in precipitates with VES-1.

3.6. Elemental Composition Test: EDS Analysis

An Evex Mini Scanning Electron Microscope (SEM) with a MSC-1000 Mini-Sputter Coater and Energy Dispersive X-ray Spectroscopy (EDS) was used to analyze the elemental compositions of selected precipitates from samples.

We noticed that Fe (III) could form precipitates with VES-1 at a relatively high concentration (higher than 4,000 ppm). The precipitates at the initial Fe (III) concentration of 6,000 ppm were taken and EDS was applied to exam the elemental composition. The resulting spectrum is displayed as follows:

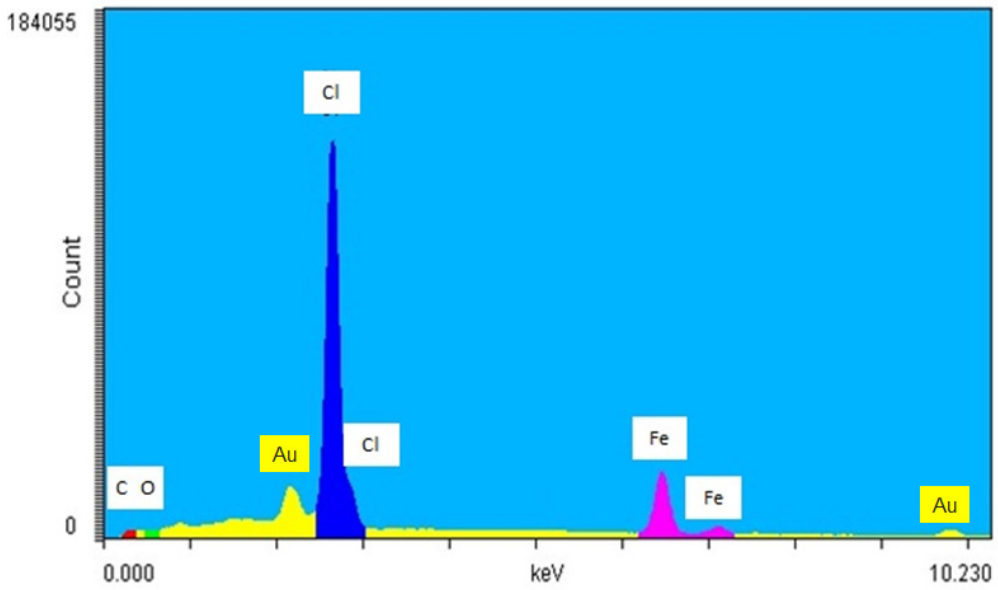

Fig. 18—EDS spectrum of the precipitate from VES-1-based acid with 6,000 ppm of Fe (III).

As shown in **Fig. 18**, the precipitate contains the element of carbon (C), oxygen (O), chlorine (Cl), and iron (Fe). It is obvious that the only source of C and O is the VES-1 and the only source of Fe is $FeCl_3$. Chlorine could be sourced from both $FeCl_3$ and HCl. As a result, there is strong evidence that the precipitate from the sample of VES-1 acid with 6,000 ppm Fe (III) is a complex containing both VES-1 and Fe (III).

At the same time, there is an interesting phenomenon: in this precipitated complex, the mole ratio between Fe and Cl is 1:3.90. We will discuss this phenomenon in the next paragraph.

3.7. Reaction Mechanism

As mentioned above, Al-Nakhli et al. (2008) presented an interesting experimental result as shown in **Fig. 19**:

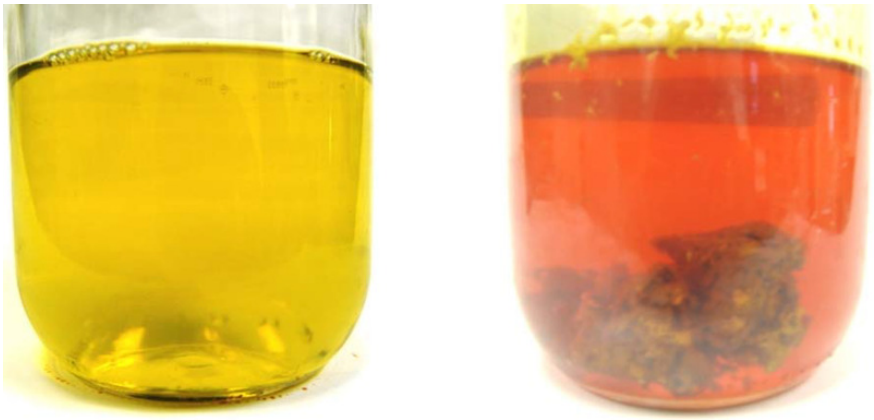

Fig. 19—VES-based acid with 6 vol% VES and 10,000 ppm Fe (III) showed different results with different HCl concentrations: 3 wt% (left) and 20 wt% (right)

In the samples above, both solutions contained 6 vol% of VES and 10,000 ppm of Fe (III). However, the results were different when concentrations of HCl were different. In the sample containing 3 wt% HCl, the solution remained clear in light yellow and there were no precipitates. Simultaneously, at the beginning of this study, VES-1-based acids with 4 vol% VES and 3 wt% HCl were also displayed with no phase separation nor precipitation, and the apparent viscosities of these VES-based acids did not change much with the increase of Fe (III) concentrations while in the sample with 20 wt% HCl, the color of the sample turned orange yellow and brown precipitates were observed at the bottom.

It is obvious that during the interaction between VES and Fe (III), the concentration of HCl also plays an important role.

As shown in **Eq. 4**, in a strong acidic environment (pH lower than 2), the VES-1 will be protonated and will become positively charged in total.

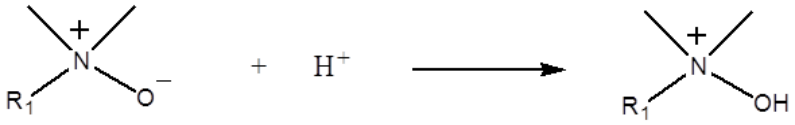

(4)

As shown in **Eq. 5**, both Fe (III) and the VES are positively charged. So it is easy to come to the conclusion that there is no interaction between them due to the electrostatic repulsion.

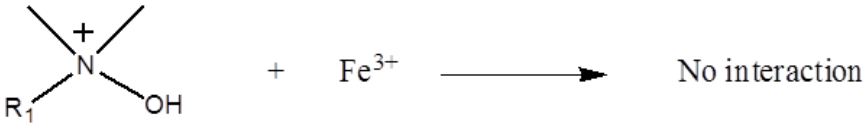

(5)

However, Fe (III) can react with chloride ions in aqueous solution to generate different forms of Fe (III)-chloride complexes. The reaction functions are expressed as

follows, and the reaction constants are denoted as K_1, K_2, K_3, and K_4 respectively (Gamlen and Jordan 1953).

$$Fe^{3+} + Cl^- \rightarrow [FeCl]^{2+} \qquad K_1 = \frac{[[FeCl]^{2+}]}{[Fe^{3+}]\times[Cl^-]} \tag{6}$$

$$[FeCl]^{2+} + Cl^- \rightarrow [FeCl_2]^+ \qquad K_2 = \frac{[[FeCl_2]^+]}{[[FeCl]^{2+}]\times[Cl^-]} \tag{7}$$

$$[FeCl_2]^+ + Cl^- \rightarrow FeCl_3 \qquad K_3 = \frac{[FeCl_3]}{[[FeCl_2]^+]\times[Cl^-]} \tag{8}$$

$$FeCl_3 + Cl^- \rightarrow [FeCl_4]^- \qquad K_4 = \frac{[[FeCl_4]^-]}{[FeCl_3]\times[Cl^-]} \tag{9}$$

In a Fe (III) solution with a relatively low concentration of HCl (0.002 mol/l), **Eq. 6** is the most preferred reaction with the highest K_1 value at 4.2 (as shown in **Table 2**, Rabinowitch and Stockmayer 1942; Nachtrieb and Conway 1948; Gamlen and Jordan 1953). With increasing concentration of HCl, the amount of $[FeCl_2]^+$ and $FeCl_3$ increase. When the concentration of HCl is higher than 2 mol/l, **Eq. 9** starts. While with a HCl concentration higher than 8 mol/l (up to 11.5 mol/l), the $[FeCl_2]^+$, $FeCl_3$ and $[FeCl_4]^-$ are the only three complexes presented in the solution.

Table 2—Different K Values in Various Concentration HCl Solutions.

HCl concentration (mol/l)	$\mathbf{K_1}$	$\mathbf{K_2}$	$\mathbf{K_3}$	$\mathbf{K_4}$
0.002	4.2	1.3	0.04	–
2	5.7	2.0	0.87	–
8	–	–	0.73	0.105

As shown in **Eq. 10**, when high concentration of HCl exists along with Fe (III), the Fe (III) can react with the Cl^- in the solution to form a negatively charged complex, $[FeCl_4]^-$ (Sharma 1974).

$$Fe^{3+} + 4Cl^- \rightleftharpoons FeCl_4^- \quad (10)$$

In this study, 20 wt% HCl was used which is equal to about 6 mol/l in concentration. At this concentration of HCl, the process in **Eq. 10** has a great tendency to occur. As a result, when the positively charged VES solution is mixed with acid containing $[FeCl_4]^-$, a coordinative bond between the positive center (N) and the negative center ($[FeCl_4]^-$) will be formed (as shown in **Eq. 11**). And, such a reaction between VES and $[FeCl_4]^-$ can lead to the breakage of the reaction equilibrium of **Eq. 10** and to the generation of more $[FeCl_4]^-$ to react with VES. The formation of this coordinative bond affords a product which could lead to an increasing apparent viscosity, phase separation, or precipitation in samples. This is the reason why we noticed that the mole ratio between Fe and Cl is almost 1:4 (1:3.90 according to the experimental results) in the EDS results of the precipitates.

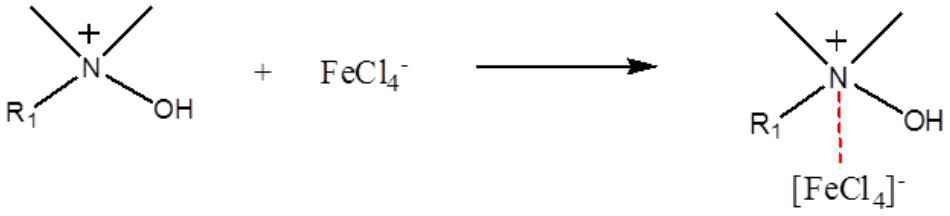

(11)

CHAPTER IV

PROPERTY MEASUREMENTS OF VES-2-BASED ACIDS AND REACTION MECHANISMS

4.1. Sample Preparation: VES-2 with 20 wt% HCl

All samples contained 4 vol% VES-2, 20 wt% HCl, and various Fe (III) concentrations at a total volume of 40 cm^3.

1. A 50 cm^3 test tube was filled with weighted $FeCl_3$ powder, and a calculated volume of DI water was injected to make a homogenous solution.

2. HCl (37 wt%, 21.6 cm^3) was measured and transferred into the tube followed by addition of 1.6 cm^3 VES-2.

3. DI water was added until the total volume of the sample reached 40 cm^3.

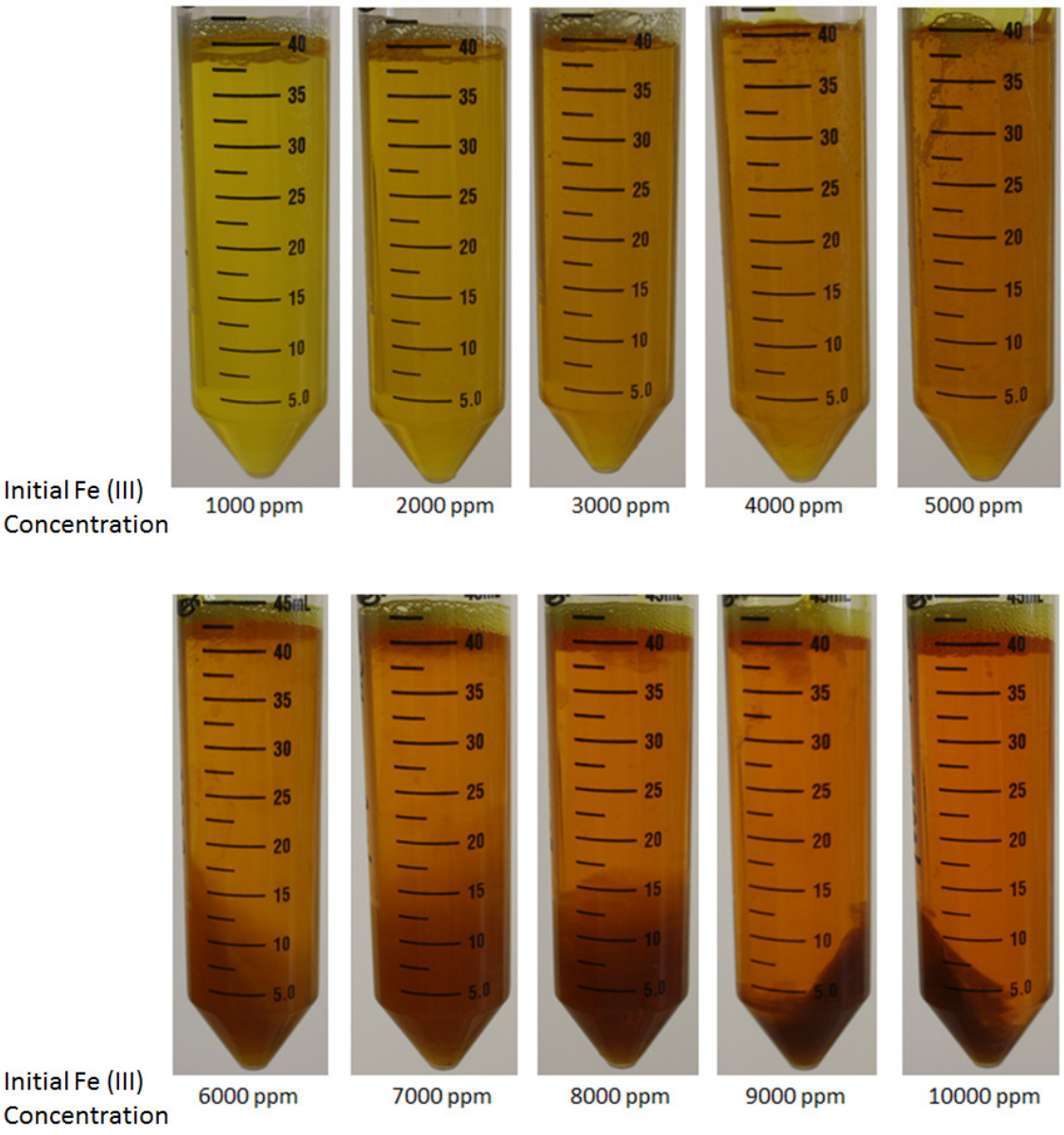

Fig. 20—Samples of VES-2-based acids: 4 vol% VES-2, 20 wt% HCl, and various concentrations of Fe (III). Freshly prepared at room temperature.

The effect of different Fe (III) concentrations on the freshly prepared VES-2 acid system at room temperature were shown in **Fig. 20**. When Fe (III) concentration was no more than 5,000 ppm, the solution remained clear while the color changed from light yellow to dark yellow. At the same time, tiny precipitates were suspended in solution making the sample appear murky. When the Fe (III) concentration was higher than 6,000 ppm, brown precipitates formed in a dark yellow solution.

4.2. Apparent Viscosity Measurements

The apparent viscosity of VES-2-based acid systems without Fe (III) is very low (about 3 cp at room temperature at a shear rate of 100 s^{-1}). As shown in **Fig. 21**, the apparent viscosity of VES-2 solutions increased quickly from 2.6 to 131 cp when Fe (III) concentration increased from 0 to 2,300 ppm. After that, the apparent viscosity of the sample decreased dramatically back to less than 5 cp at higher Fe (III) concentrations.

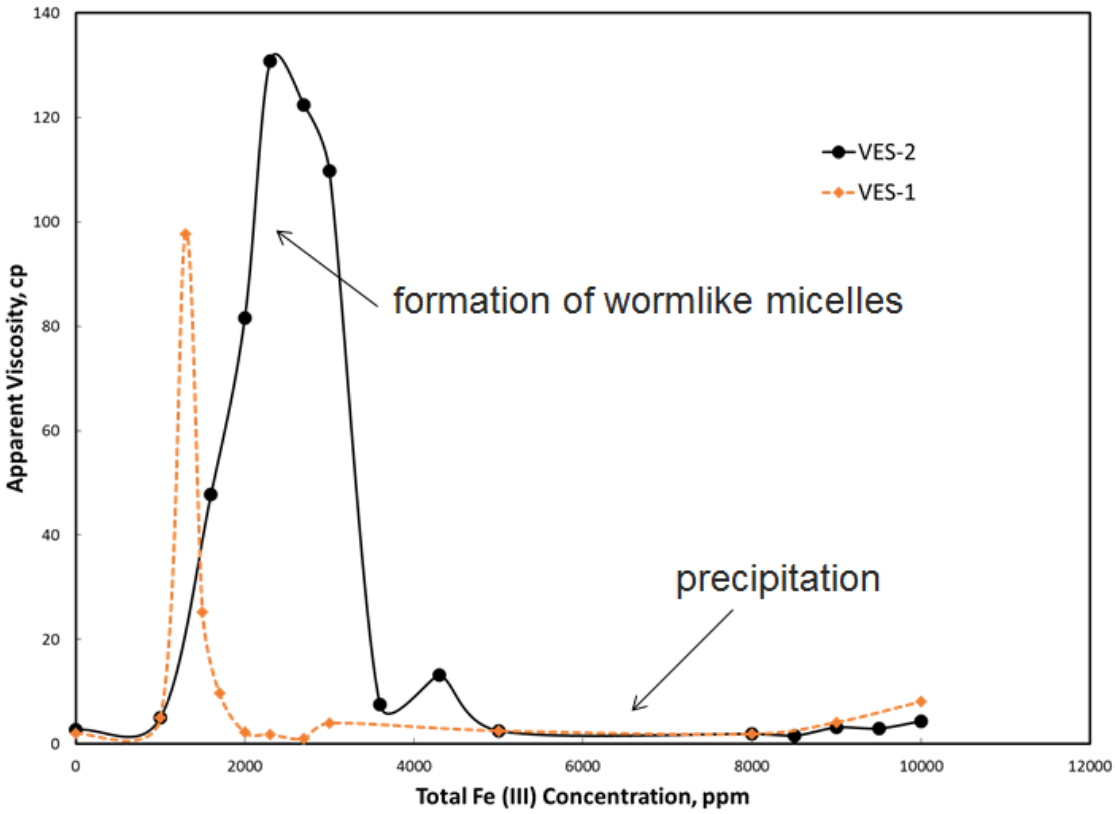

Fig. 21—Apparent viscosity of VES-2 solutions at different concentrations of Fe (III) at room temperature and at a shear rate of 100 s^{-1}. VES-2-based acids showed different apparent viscosities because of various Fe (III) concentrations at a HCl concentration of 20 wt%.

Compared to the observations of all VES-2 samples, when the Fe (III) concentration was no more than 2,300 ppm, the solution was clear and much more viscous than the sample without Fe (III). The apparent viscosity could increase to as high as 131 cp. While the Fe (III) concentration was higher than 2,300 ppm, tiny precipitates were observed and the apparent viscosity of the sample decreased quickly to about 10 cp

at a Fe (III) concentration of 3,600 ppm. Then, even as the Fe (III) concentration increased to as high as 10,000 ppm, the apparent viscosity of the sample kept lower than 10 cp, and obvious precipitates were obtained when the Fe (III) concentration was higher than 5,000 ppm.

This change in apparent viscosity of all samples implies the reaction between Fe (III) and VES-2. At low Fe (III) concentrations, long rod-shape micelles formed, leading to the dramatic increase of apparent viscosity. As a result, during the acid treatment, it would be difficult to inject the VES-based acid and the reaction rate of acidizing would be lowered. At the same time, in the environment with high Fe (III) concentrations (higher than 5,000 ppm), the formation of precipitates may lead to possible formation damage.

Compared to VES-1 samples, in the existence of Fe (III), VES-2 samples could lead to a higher maximum apparent viscosity and could sustain higher Fe (III) concentrations. In VES-1-based acids, phase separation was observed when the Fe (III) concentration was higher than 1,500 ppm while precipitates were obtained when the Fe (III) concentration was higher than 4,000 ppm. However, in VES-2-based acids, there was no phase separation and the precipitation started when the Fe (III) concentration was higher than 5,000 ppm.

4.3. Concentration Measurements: VES Concentrations

The concentrations of VES-2 in all samples were titrated via the two-phase titration method and the results were plotted.

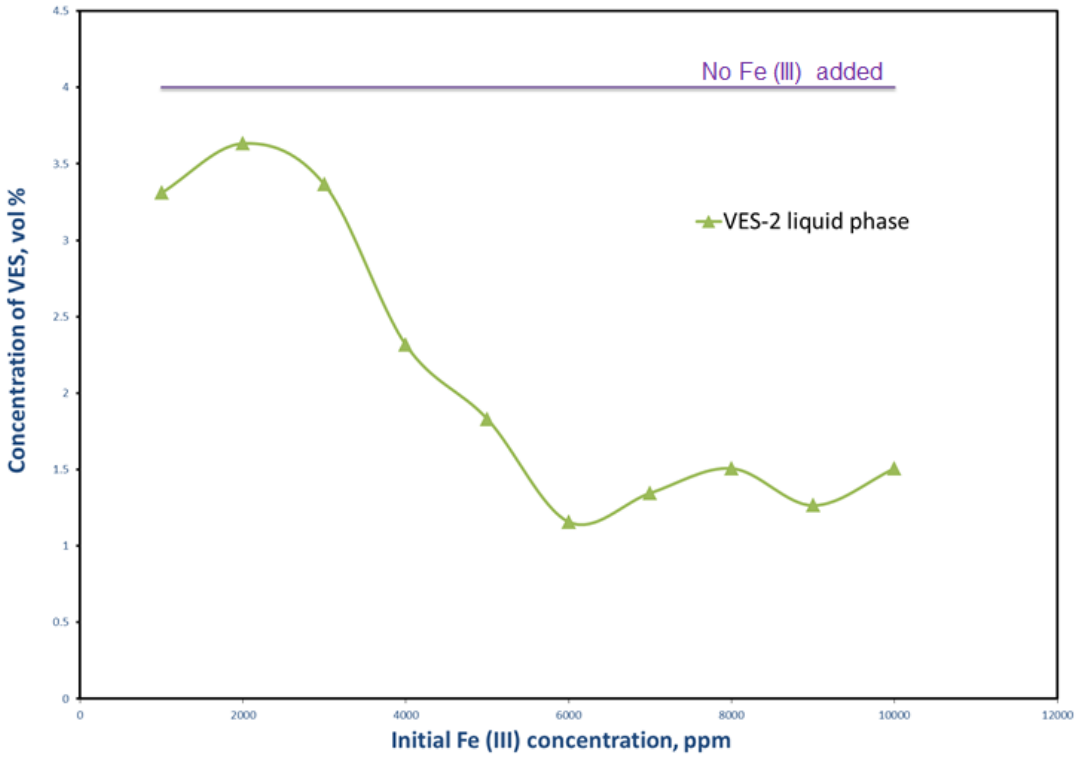

Fig. 22— Concentrations of VES-2 in the presence of various concentrations of Fe (III) at room temperature, freshly prepared.

As shown in **Fig. 22**, the concentrations of VES-2 were titrated and plotted. All of these samples can be divided into three subgroups based on differing concentrations of Fe (III).

The sample at the Fe (III) concentration of 1,000, 2,000, and 3,000 ppm were all light yellow clear solutions. VES-2 remained in the solution without precipitation nor phase separation.

Both colors of the samples at the Fe (III) concentration of 4,000 and 5,000 ppm became darker than samples containing less Fe (III) and the solutions became murky. This indicated the formation of small precipitates. Therefore, the concentration of VES-2 in solution had continued to decrease.

Samples at the Fe (III) concentration of 6,000 ppm and higher formed brown precipitates at the bottom of a dark yellow solution. The concentration of VES-2 had further decreased to less than 1.5 vol%.

These results indicated the presence of interactions between Fe (III) and VES-2. In the environment of high Fe (III) concentrations (above 5,000 ppm), such interaction can even lead to precipitation, which may also result in severe formation damage.

4.4. Concentration Measurements: Fe (III) Concentrations

Fig. 23 shows the concentration of Fe (III) in solutions of freshly prepared VES-2 acid samples. As discussed above, each of these samples can be divided into three subgroups. At the initial Fe (III) concentration of 1,000 to 3,000 ppm, sample solutions remained clear while from 4,000 to 5,000 ppm, the solutions became murky, which indicated the formation of small precipitates. When the initial Fe (III) concentration was higher than 6,000 ppm, brown precipitates were obtained at the bottom of solution. So there was a sudden Fe (III) concentration drop shown in the graph from 5,000 to 6,000 ppm. That means the precipitation took more Fe (III) ions from the solution, which is also evidence of the interaction between VES-2 and Fe (III).

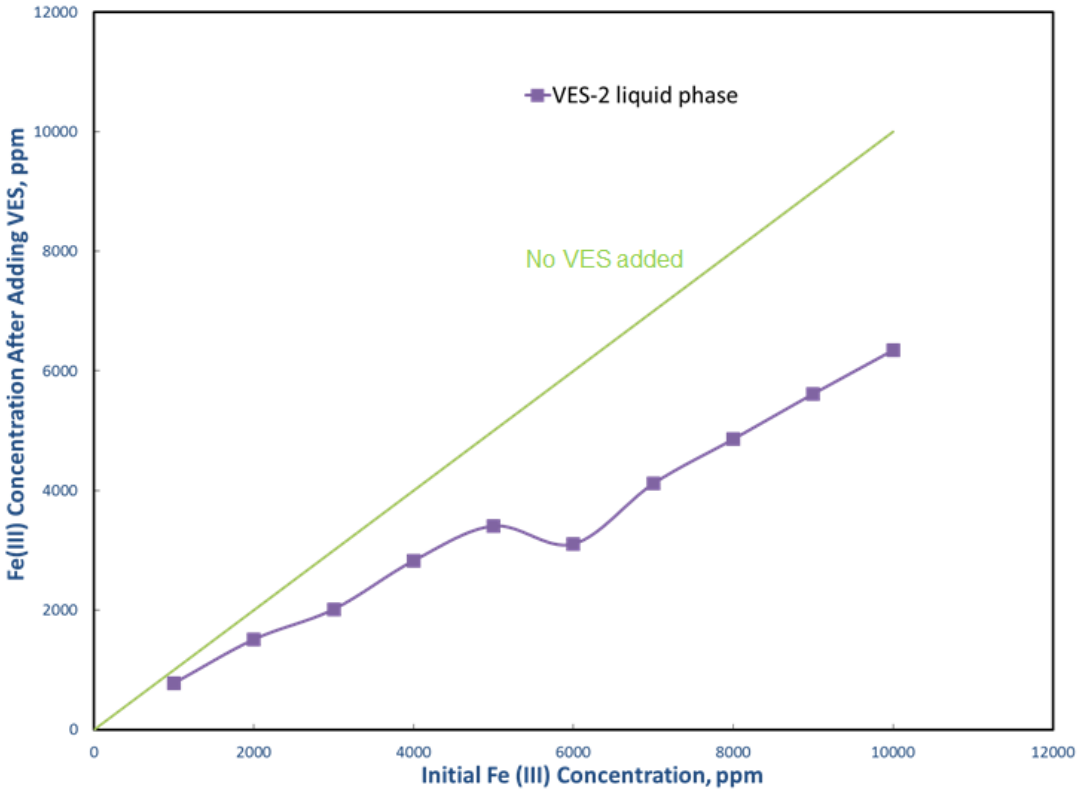

Fig. 23— Fe (III) concentrations in the liquid phases in all VES-2-based acid samples at room temperature.

4.5. Element Composition Test: EDS Analysis

An Evex Mini Scanning Electron Microscope (SEM) with a MSC-1000 Mini-Sputter Coater and Energy Dispersive X-ray Spectroscopy (EDS) was used to analyze the elemental composition of selected precipitates from samples.

Precipitates of VES-2, at the Fe (III) concentration of 6,000 ppm, were taken and EDS was used to examine the elemental composition. The resulting spectrum is displayed as follows:

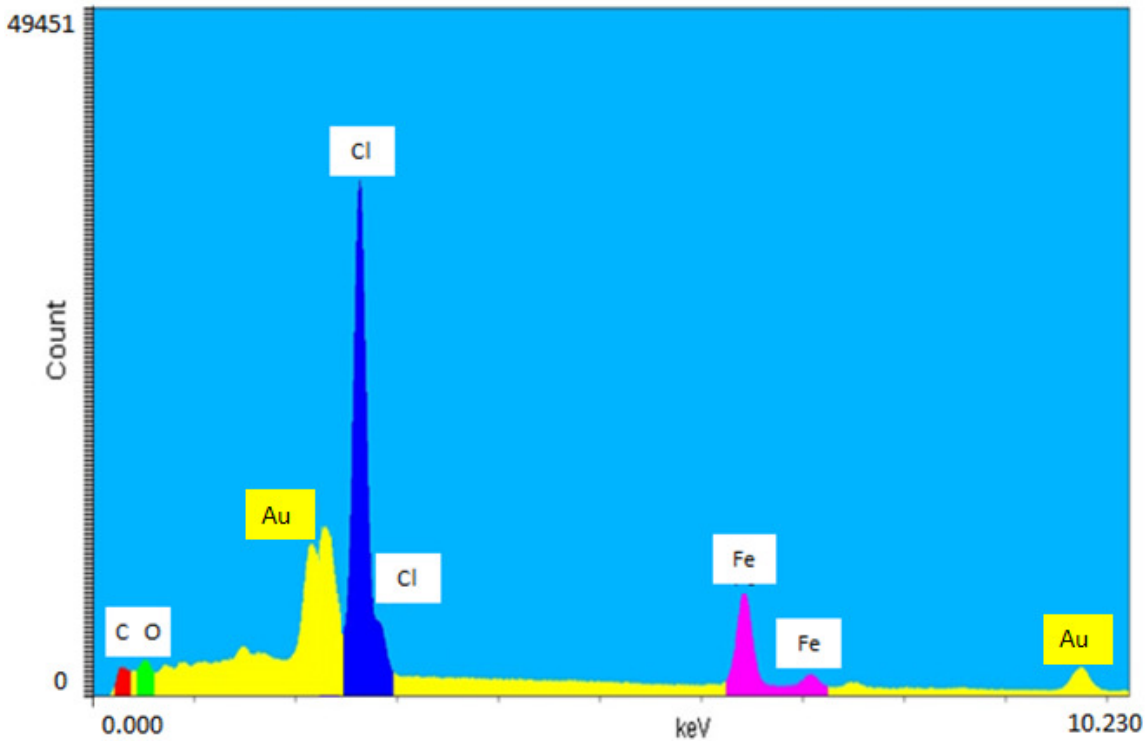

Fig. 24—EDS analysis result of the precipitate from VES-2-based acid with 6,000 ppm of Fe (III).

As shown in **Fig. 24**, the precipitate contained the element of carbon (C), oxygen (O), chlorine (Cl), and iron (Fe). It is obvious that the only source of C and O is the VES-2 and the only source of Fe is $FeCl_3$. Chlorine could be sourced from both $FeCl_3$ and HCl. As a result, we can conclude that the precipitate from the sample of VES-2 acid with 6,000 ppm Fe (III) is a complex containing both VES-2 and Fe (III).

The observation of C, O, Cl, and Fe from precipitates of VES-2 samples directly indicates that VES-2 can react with Fe (III) and form precipitate when the Fe (III) concentration is high enough.

Similar to the mechanism described in **Eq. 9**, it is obvious VES-2 could form a complex with $[FeCl_4]^-$ as shown in **Fig. 25**.

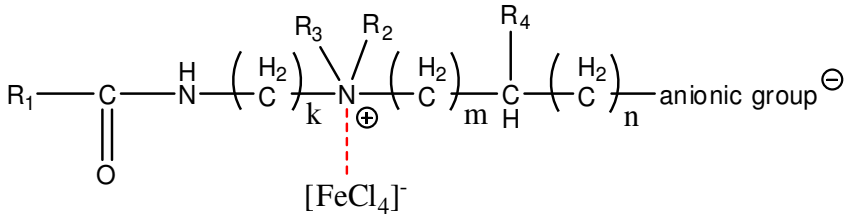

Fig. 25—Molecular structure of the complex formed from the reaction between VES-2 and Fe (III).

Interestingly, we noticed the mole ratio between Fe and Cl is 1:3.74 from the EDS spectrum, which is very close to the theoretical mole ratio among these elements (1:4) in the complex shown in **Fig. 25**. This provides strong evidence on our proposed reaction mechanism.

CHAPTER V

PROTECTION EFFECT OF CHELATING AGENTS ON VES-BASED ACID

5.1. Mechanism of the Reaction between Chelating Agents and Metal Ions

Chelating agents are widely used to bind different kinds of metal ions in solution. After the chelating reaction, free metal ions could be bonded to the chelating agent and may not be easily released. In previous work, many chelating agents, such as ethylenediaminetetraacetic acid (EDTA), nitrilotriacetic acid (NTA), citric acid and so on have been studied.

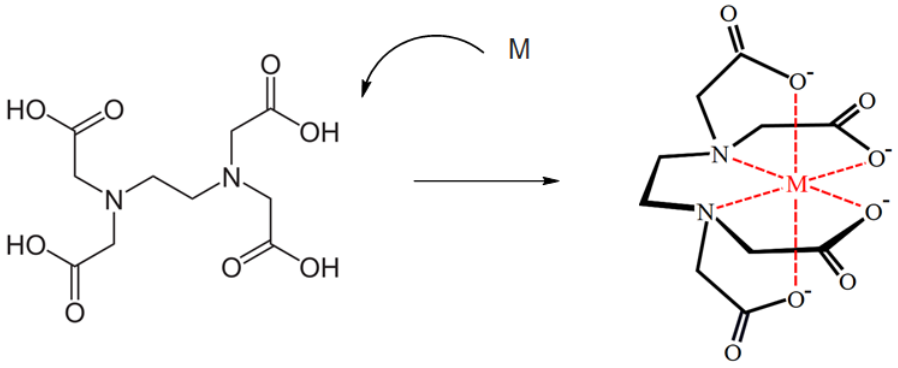

(12)

The general idea of how a chelating agent reacts with a metal ion in solution is shown in **Eq. 12** with EDTA as the example. After mixing the chelating agent and the metal ions, several coordinative bonds are formed between the metal ions and the EDTA. As a result, the free metal ion is "grabbed" by the EDTA molecule and will not be easily released to react with other reagents in solution.

The chelation between Fe (III) and EDTA could be one possible reaction mechanism. As shown in **Fig. 26**, the reaction constant between EDTA and Fe (III) is much larger than that between Cl^- and Fe (III). As a result, when EDTA and Cl^- exist in

the solution at the same time with Fe (III), Fe (III) can barely react with Cl^- to form the $[FeCl_4]^-$ complex needed to interact with VES. In this way, VES in the acids could be protected from the impact of Fe (III).

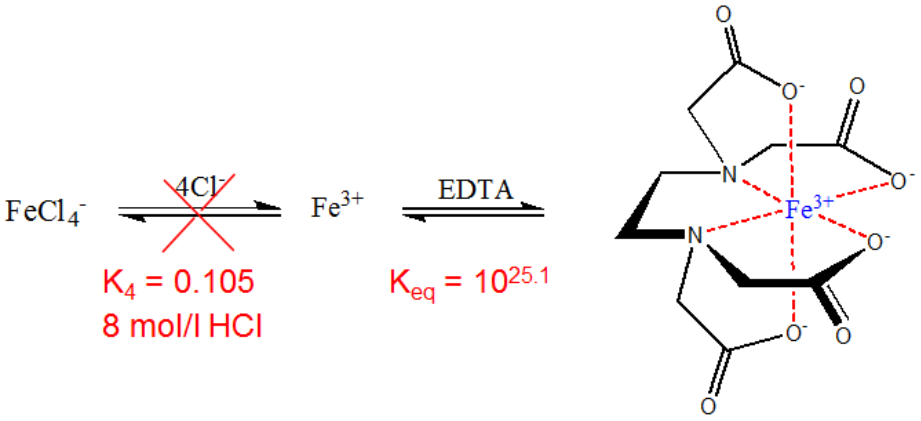

Fig. 26—Fe (III) has the tendency to react with EDTA rather than Cl^- because of the much larger reaction constant.

The electrostatic interactions could be another possible reaction mechanism. When EDTA was used in a strong acidic environment, it would be protonated to form a positively charged $[EDTA\text{-}H_2]^{2+}$ complex (as shown in **Eq. 13**). There would be an electrostatic interaction between this $[EDTA\text{-}H_2]^{2+}$ and the negatively charged $[FeCl_4]^-$ complex. Therefore, the impact of Fe (III) on the VES could be reduced.

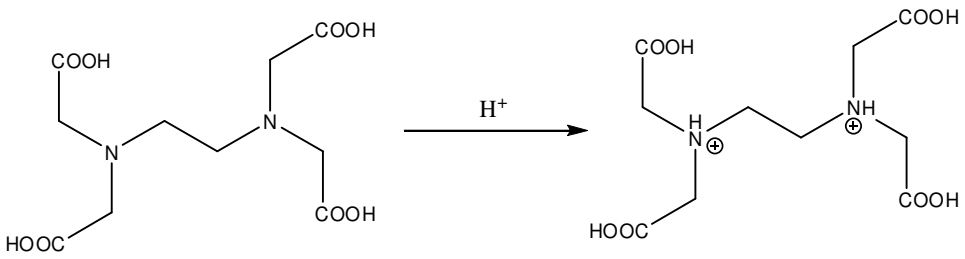

(13)

However, several problems may present under certain conditions. The most serious problem of using EDTA or NTA is the solubility in strong acids. When the solution has a pH value of lower than 2, only small amount of EDTA or NTA can be dissolved. At the same time, citric acid can react with Ca^{2+} in spent acid to form a precipitate which may lead to potential formation damage.

In order to examine the effects of different chelating agents, L-glutamic acid N,N-diacetic acid (GLDA) and hydroxyethylenediaminetriacetic acid (HEDTA) (as shown in **Fig. 27**) were considered in this study and their salts, GLDA-NaH_3 and HEDTA-NaH_2, were used. Both of these two chelating agents show good solubility, even in strong acidic solutions.

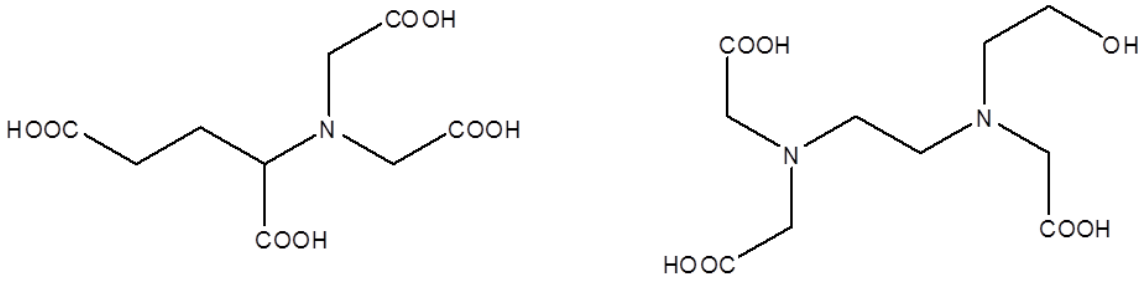

Fig. 27—Molecular structures of GLDA (left) and HEDTA (right).

As discussed above, the existence of Fe (III) can affect the VES-based acid system due to the interaction between Fe (III) and VES. Such interaction may lead to viscosity changes, phase separation, or precipitation. The idea of using chelating agents to reduce the effect of Fe (III) in VES-based acid systems was proposed and examined via viscosity measurements of each sample. A coreflood was also used to determine the effect of chelating agents on the VES-based acids. In each sample, GLDA-NaH_3 and

HEDTA-NaH_2 were mixed into both VES-1 and VES-2 solutions, and then $FeCl_3$ was added. The mole ratio between the chelating agents and the Fe (III) was 1:1.

5.2. Sample Preparation: VES-2 and 20 wt% HCl with Chelating Agents

Each sample contained 4 vol% VES-2, 20 wt% HCl, various Fe (III) concentrations, and a chelating agent, which was 1:1 mole ratio to Fe (III), at a total volume of 40 cm^3.

The following procedures were followed to prepare each sample:

1. A 50 cm^3 beaker was filled with weighted $FeCl_3$ powder and calculated volume of DI water was added to make a homogenous solution.

2. Calculated volume of 37 wt% HCl was measured and transferred into another 50 cm^3 beaker and 1.6 cm^3 VES was slowly added during stirring.

3. 1:1 mole ratio of the chelating agent (GLDA-NaH_3 or HEDTA-NaH_2) was added into the VES-HCl solution during stirring.

4. The prepared $FeCl_3$ solution was added drop by drop into the VES-HCl solution during stirring.

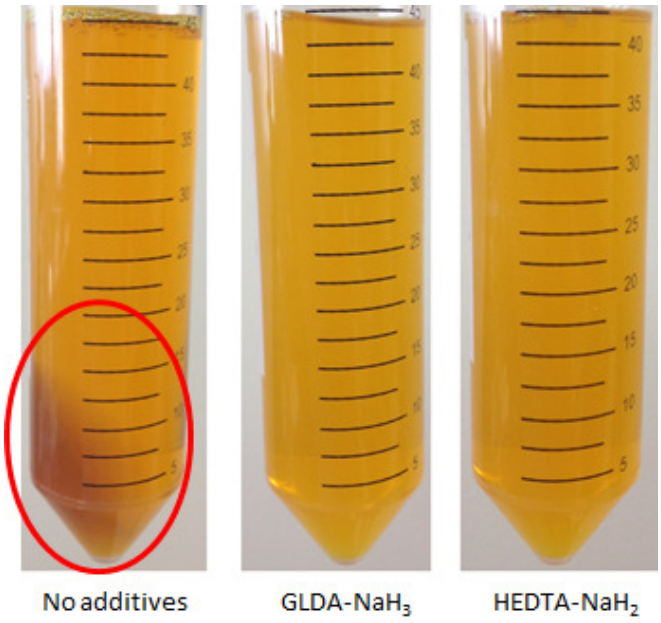

Fig. 28—VES-2-based acids: 4 vol% VES-2, 6,000 ppm Fe (III), and 20 wt% HCl. If no chelating agent was added, brown gel-like materials were noted at the bottom (left). With adding chelating agents [1:1 mole ratio to Fe (III)] GLDA-NaH_3 (middle) or HEDTA-NaH_2 (right), no precipitates were noticed.

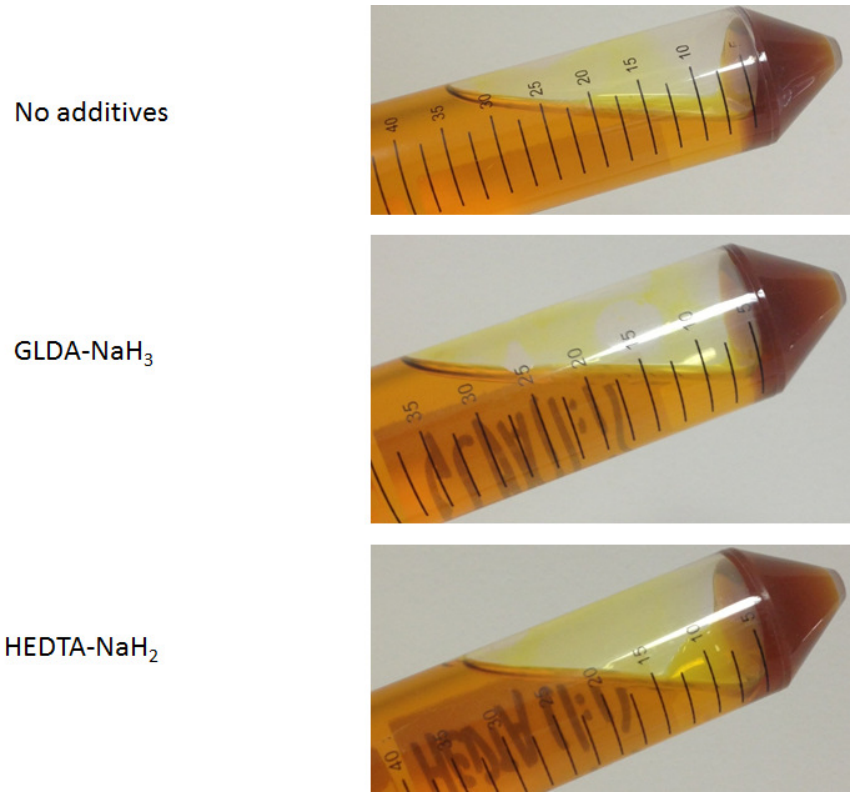

Fig. 29— VES-2-based acids: 4 vol% VES-2, 8,000 ppm Fe (III), and 20 wt% HCl. If no chelating agent was added, brown gel-like materials were obtained at the bottom (top). With adding chelating agents [1:1 mole ratio to Fe (III)] GLDA-NaH_3 (middle) or HEDTA-NaH_2 (right), brown gel-like materials were also noticed at the bottom.

As shown in **Fig. 28**, when Fe (III) concentration was 6,000 ppm, as discussed above, if no chelating agent was added, brown gel-like materials were noted at the bottom of the test tube. However, with adding chelating agents [1:1 mole ratio to Fe (III)] GLDA-NaH_3 or HEDTA-NaH_2, no precipitates were noticed. It is obvious that the

chelating agent (GLDA-NaH_3 and HEDTA-NaH_2) minimized the formation of precipitates, which reduced the possibility of formation damage.

As shown in **Fig. 29**, when the Fe (III) concentration increased to 8,000 ppm, even with 1:1 mole ratio of chelating agent (GLDA-NaH_3 or HEDTA-NaH_2), brown gel-like materials were still obtained. This also indicates the usage limitation of chelating agent in this case.

5.3. Apparent Viscosity Measurements

The apparent viscosity of all VES-2 samples with both GLDA-NaH_3 and HEDTA-NaH_2 was measured at room temperature in the presence of different concentrations of Fe (III). The results at a shear rate of 100 s^{-1} were shown in **Fig. 30** and **Fig. 31**.

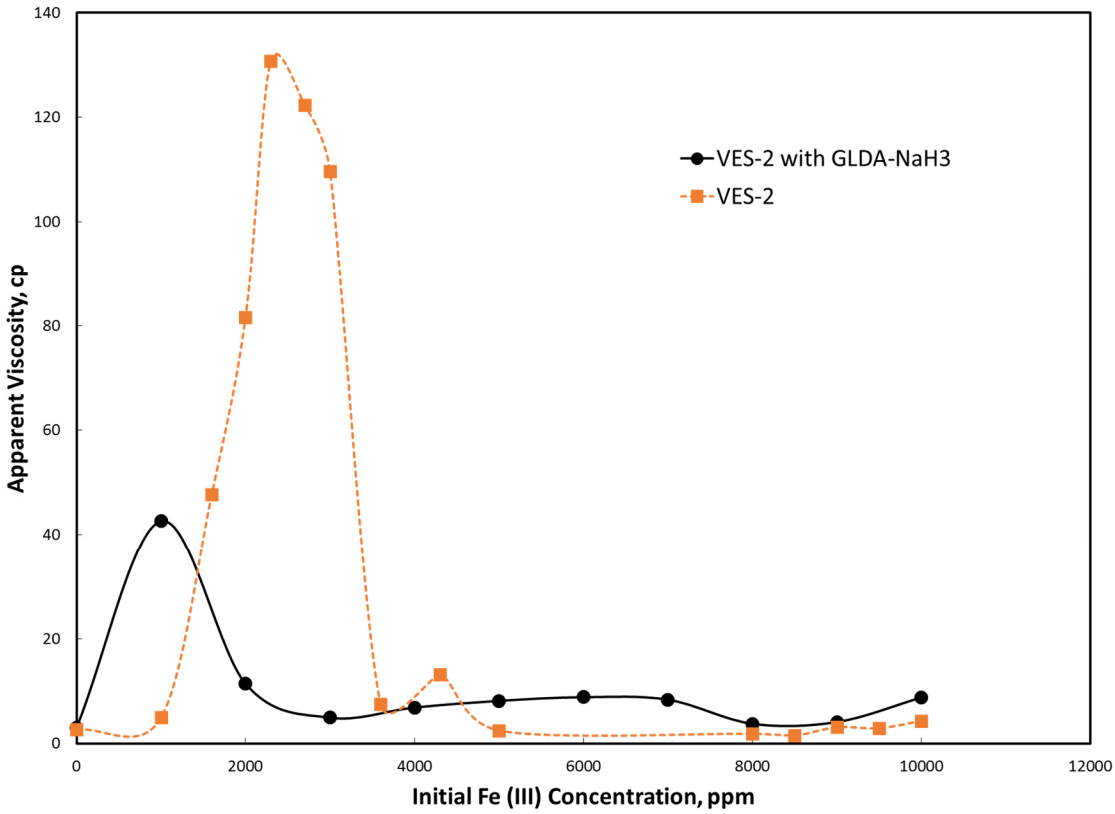

Fig. 30—Apparent viscosity of samples of VES-2-based acids (4 vol% VES-2, 20 wt% HCl, various concentrations of Fe (III), and GLDA-NaH_3 [1:1 mole ratio to Fe (III)]) at room temperature and at a shear rate of 100 s^{-1}.

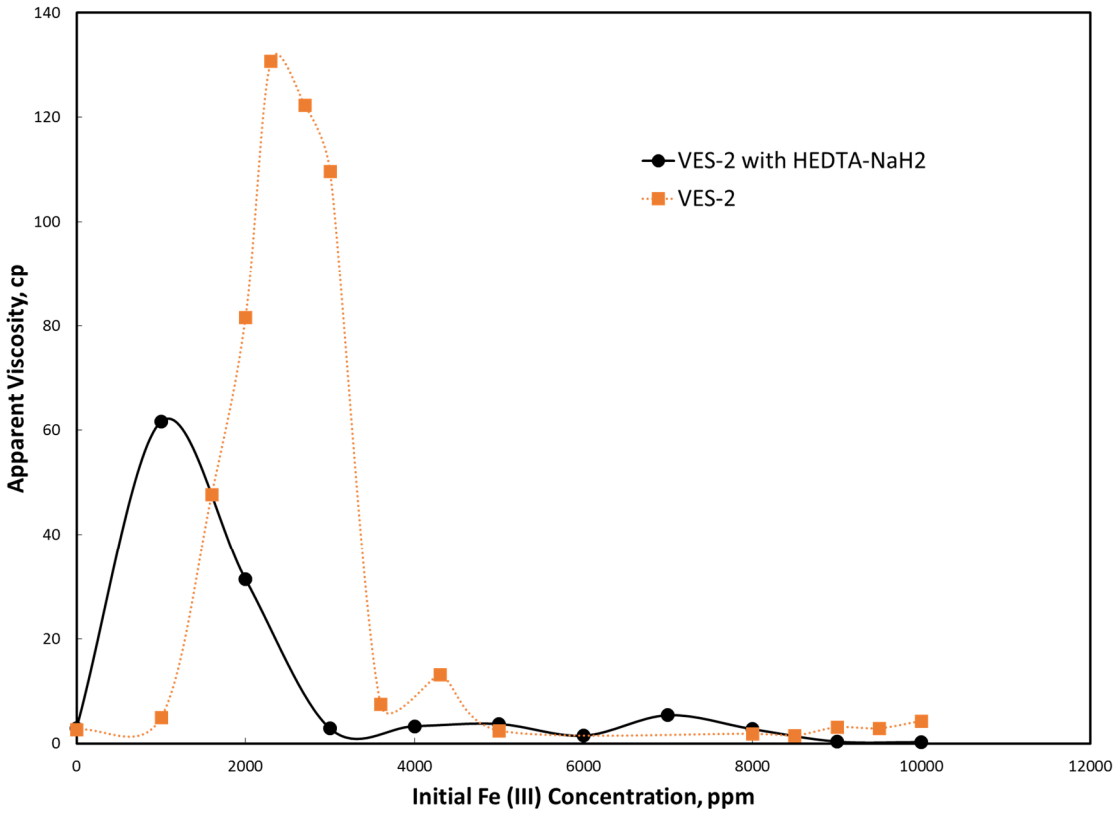

Fig. 31—Apparent viscosity of samples of VES-2-based acids (4 vol% VES-2, 20 wt% HCl, various concentrations of Fe (III), and HEDTA-NaH_2 [1:1 mole ratio to Fe (III)]) at room temperature and at a shear rate of 100 s^{-1}.

As discussed in Chapter II, if there was no Fe (III) nor chelating agent in the VES-based acids, the apparent viscosity of the solution is about 3 cp at a shear rate of 100 s^{-1} at room temperature. When in Fe (III) containing environment, if there was no phase separation or precipitation of the sample solution, the viscosity of the sample will increase significantly. The highest apparent viscosity (131 cp) was obtained when the

concentration of Fe (III) at 2,300 ppm without any chelating agent at a shear rate of 100 s^{-1} at room temperature.

However, as shown in **Fig. 30** and **Fig. 31**, both GLDA-NaH_3 and HEDTA-NaH_2 lowered the apparent viscosity of VES-2 solutions effectively. With the same shear rate at 100 s^{-1} at room temperature, in VES-2-based acid samples with GLDA-NaH_3, the highest apparent viscosity (42 cp) was reached at the Fe (III) concentration of 1,000 ppm. While in acid samples with HEDTA-NaH_2, the highest apparent viscosity (62 cp) was also reached at the Fe (III) concentration of 1,000 ppm.

It is easy to find with the addition of chelating agents, the maximum apparent viscosity was decreased. That is because the chelating agent can bond with Fe (III) ions to prevent the interaction between VES molecules and Fe (III) ions. Formation of such chelating bonds is able to "grab" Fe (III) ion in the solution, which helps to protect the VES-based systems.

On the other hand, when the concentration of Fe (III) was higher than 5,000 ppm, even with chelating agents like GLDA-NaH_3 and HEDTA-NaH_2 in the VES-based acid systems, possible formation damage because of the precipitates formed was still be observed.

VES-1-based acids were also examined with adding these two chelating agents (GLDA-NaH_3 and HEDTA-NaH_2). The apparent viscosity of all samples with various concentrations of Fe (III) and chelating agents was measured and plotted in **Fig. 32** and **Fig. 33** as follows:

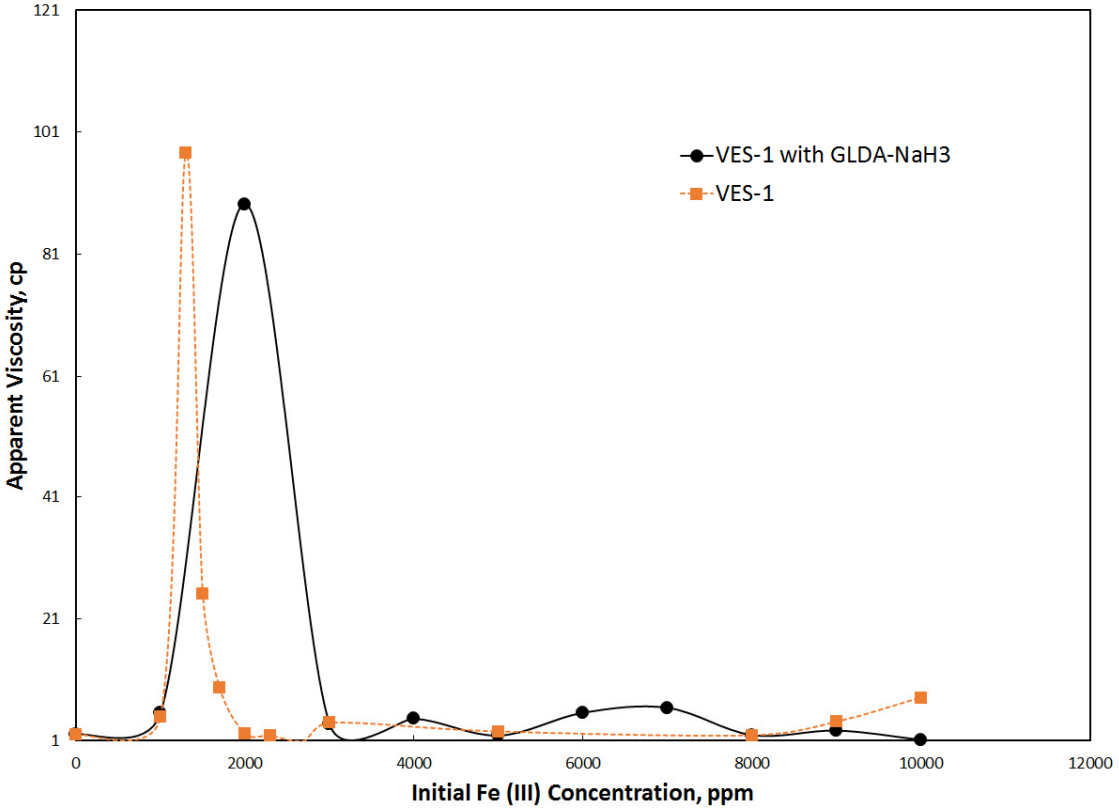

Fig. 32—Apparent viscosity of samples of VES-1-based acids at room temperature and a shear rate of 100 s^{-1}: 4 vol% VES-1, 20 wt% HCl, various concentrations of Fe (III), and GLDA-NaH_3 [1:1 mole ratio to Fe (III)].

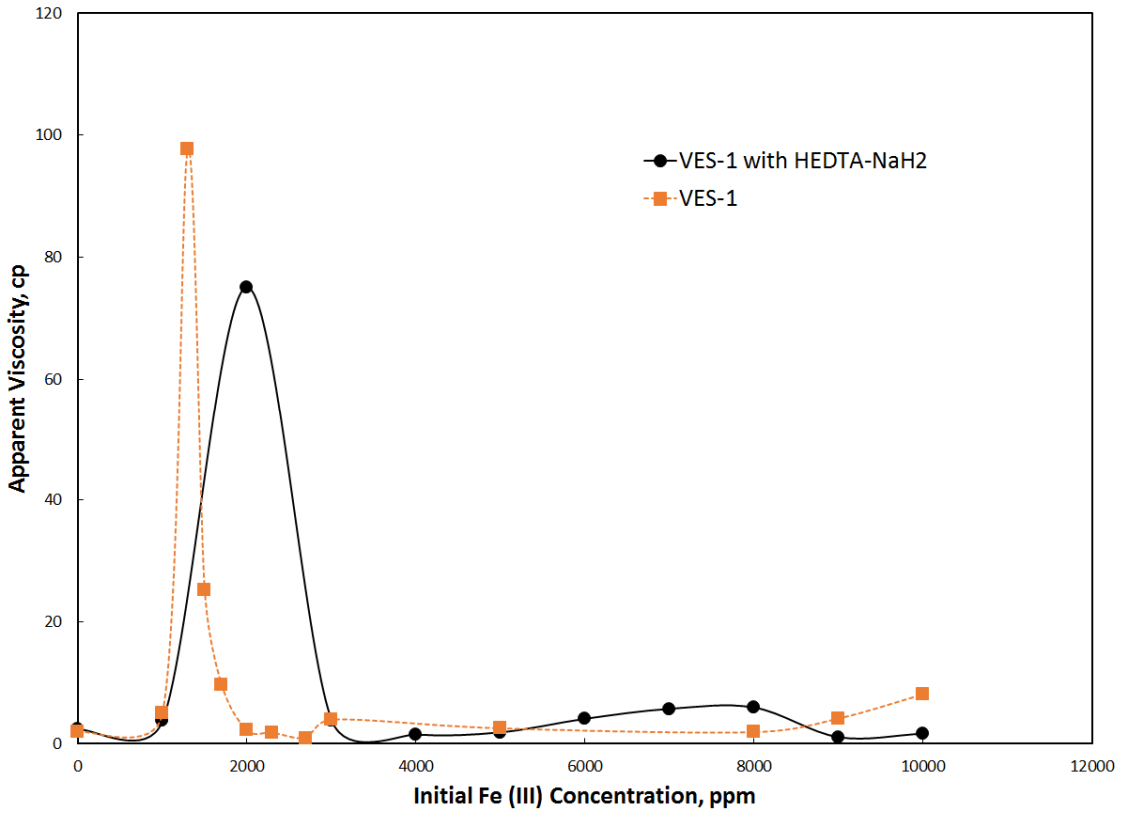

Fig. 33—Apparent viscosity of samples of VES-1-based acids at room temperature and a shear rate of 100 s^{-1}: 4 vol% VES-1, 20 wt% HCl, various concentrations of Fe (III), and HEDTA-NaH_2 [1:1 mole ratio to Fe (III)].

The apparent viscosity of VES-1-based acid solution without any chelating agent was compared with the ones with chelating agents GLDA-NaH_3 and HEDTA-NaH_2, it is noticed the maximum apparent viscosity was shown at the Fe (III) concentration of 2,000 ppm. It was noticed even with adding of chelating agents, the maximum viscosity of VES-2-based acids did not decrease much. This indicates both GLDA-NaH_3 and HEDTA-NaH_2 may not be able to prevent Fe (III) impactions in VES-1-based acids.

5.4. Coreflood Studies

Coreflood setup (as shown in **Fig. 34**) was used to study the protection effect of chelating agents on VES-based acid systems. VES-1 and chelating agent GLDA-NaH_3 were selected. The Fe (III) concentration was 2,000 ppm in all samples with a 1:1 mole ratio of GLDA-NaH_3 in 20 wt% HCl and 4 vol% VES-1 acid solutions. Indiana limestone (length: 6 inch, diameter: 1.5 inch) was used as the sample core plug. The flow rate was set at 2.5 ml/min and the experiment was performed at room temperature.

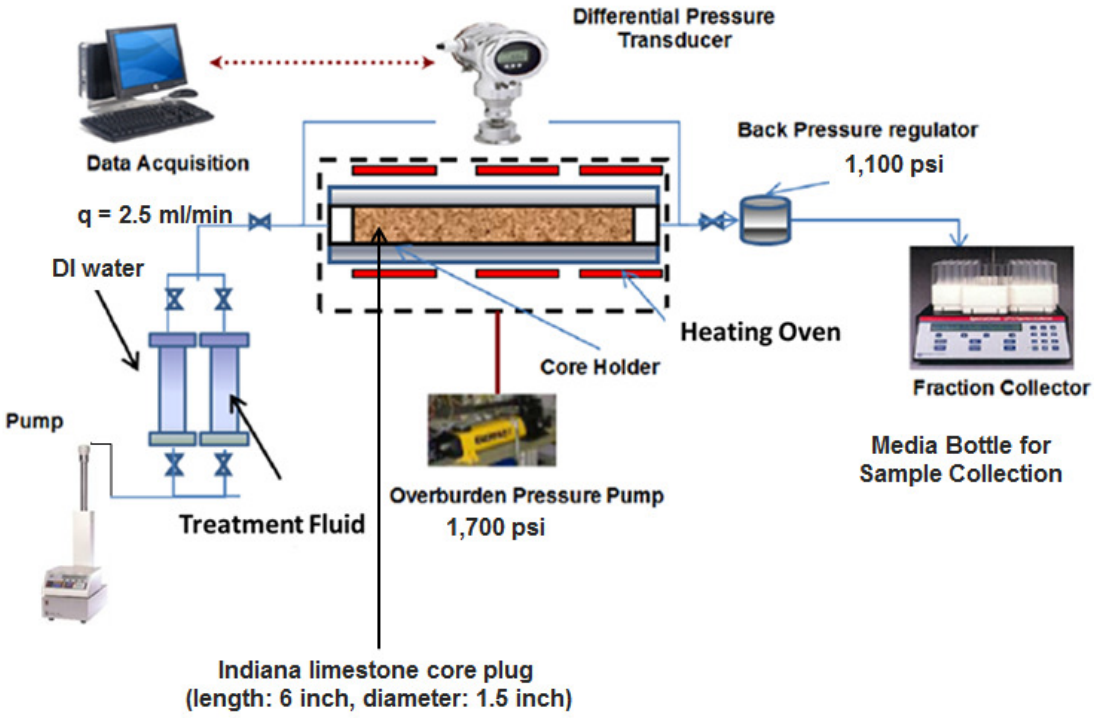

Fig. 34—Sketch model of coreflood setup equipment.

VES-1-based acid was prepared as the injection fluid:

1. A 250 cm^3 beaker was filled with weighted $FeCl_3$ powder and a calculated volume of DI water was injected to make a homogenous solution.

2. HCl (37 wt%, 50.2 cm^3) was measured and transferred into the beaker followed by addition of 4.0 cm^3 VES-1.

3. Corrosion inhibitor (CI-5, 1.0 ml) was added to the solution

4. DI water was added until the total volume of the sample reached 100 cm^3. The solution was then stirred to make it uniform.

The prepared acid solution was added to the cylinder of coreflood setup. 0.5 pore volume (15 ml) de-ionized water (DI water) was injected. Then 0.25 pore volume (7.5 ml) of the VES-1-based acid was charged. After the addition of the acid, DI water was injected from the opposite direction until the effluent was colorless with no bubbles. The pressure drop of the above produce was recorded as follows:

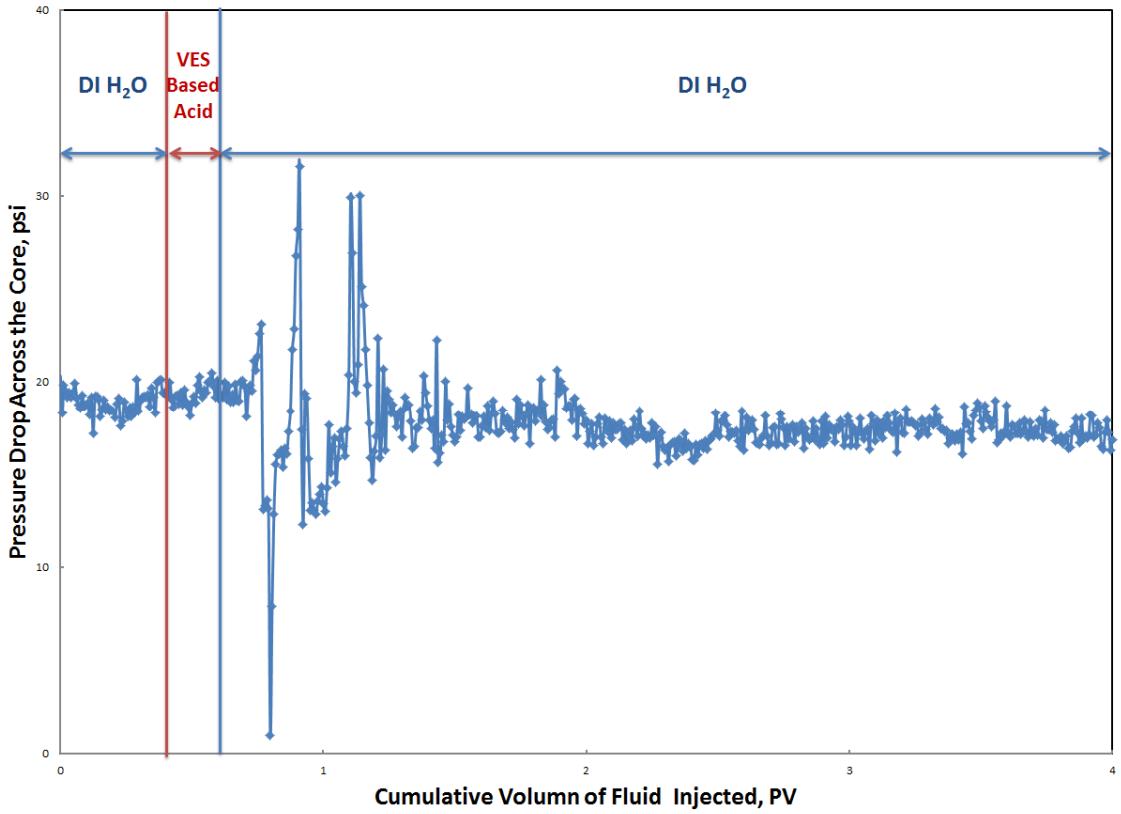

Fig. 35—Pressure drop across the core plug. VES-1-based acid [4 vol% VES-1, 20 wt% HCl, 0.5 vol% CI and 2,000 ppm Fe (III)] was injected at 2.5 ml/min at room temperature.

As shown in **Fig. 35**, the pressure drop was recorded during the experiment and the permeability of the sample core plug was calculated before and after the treatment. It turned out the permeability changed from 113 mD to 121 mD without adding any chelating agent.

At the same time, the VES-1-based acid with GLDA-NaH_3 was also prepared:

1. A 250 cm^3 beaker was charged with weighted $FeCl_3$ powder and calculated volume of DI water was added to make a homogenous solution.

2. HCl (37 wt%, 50.2 cm^3) was measured and transferred into the beaker and 4.0 cm^3 VES-1 was added.

3. The chelating agent, which is 1:1 mole ratio to Fe (III), was added into the sample beaker.

4. Corrosion inhibitor (CI-5, 1.0 ml) was added into the solution.

5. DI water was added until the total volume of the sample reached 100 cm^3. The solution was stirred to make it uniform.

Following identical procedure as discussed in previous part, the pressure drop of this treatment was recorded as in **Fig. 36**.

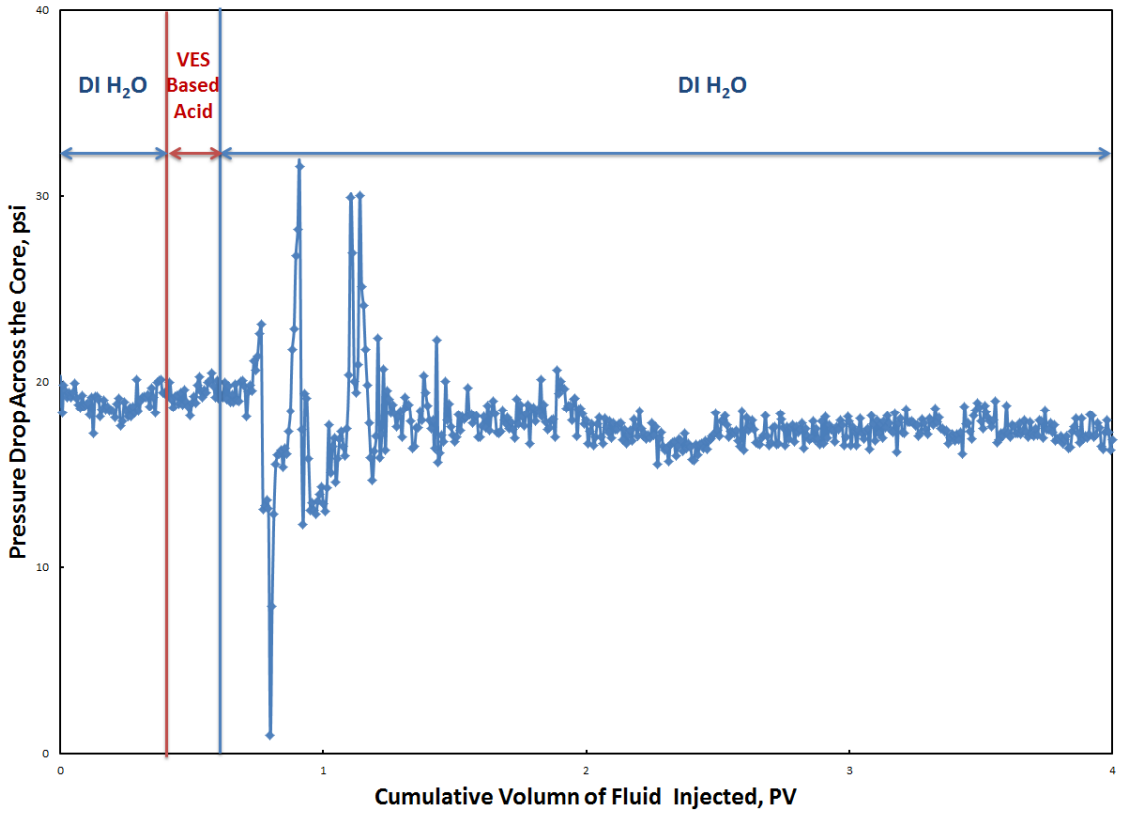

Fig. 36—Pressure drop across the core plug. VES-1-based acid (4 vol% VES-1, 20 wt% HCl, 0.5 vol% CI, 2,000 ppm Fe (III) and GLDA-NaH_3 [1:1 mole ratio to Fe (III)]) was injected at 2.5 ml/min at room temperature.

Also, the permeability of the sample core plug was measured before and after the treatment. It turned out the permeability changed from 139 mD to 152 mD with adding 1:1 mole ratio of GLDA-NaH_3.

As discussed above, the permeability of the core plug increased 7.1% by using the VES-1-based acids without GLDA-NaH_3 while the permeability of the core plug increased 9.4% after the treatment of VES-1-based acids with GLDA-NaH_3 [1:1 mole

ratio to Fe (III)]. There is no significant difference between these two treatments on the enhancement of the permeability. This result matches the apparent viscosity measurements of all VES-1-based acids samples.

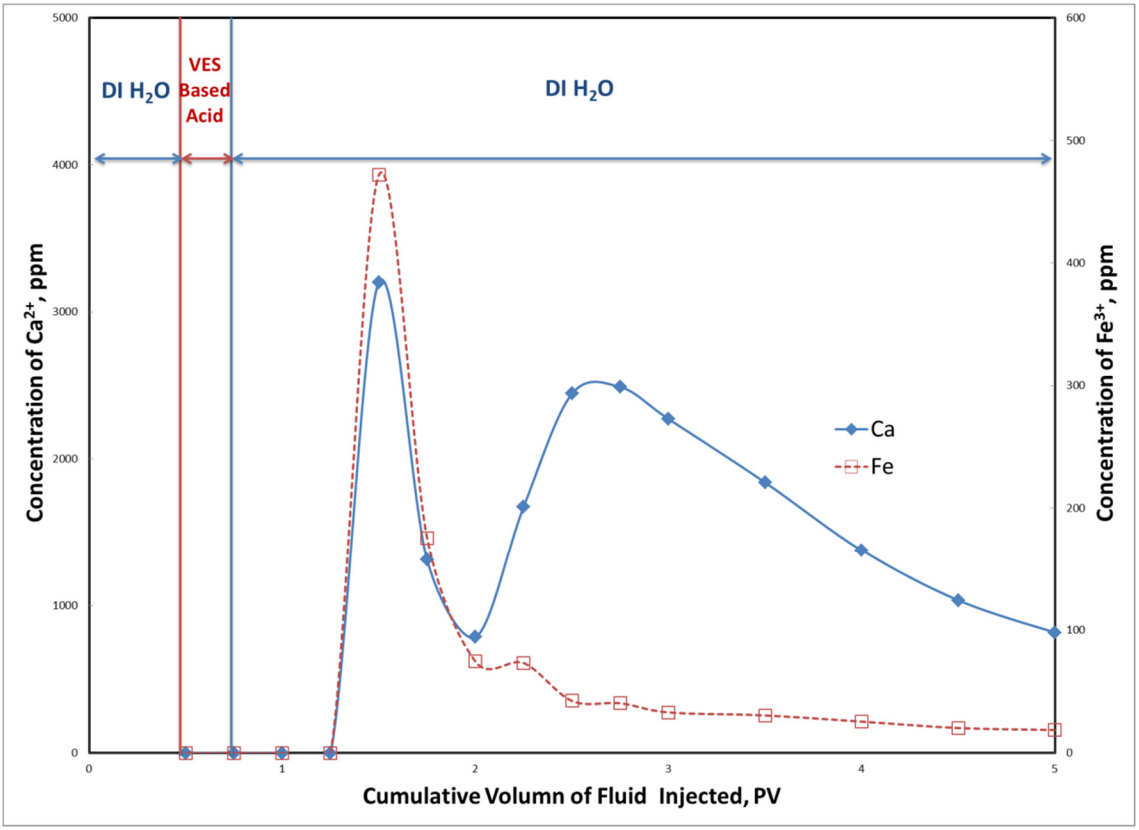

Fig. 37—Concentrations of Ca^{2+} and Fe^{3+} in effluent from the coreflood experiment. VES-1-based acid [4 vol% VES-1, 20 wt% HCl, 0.5 vol% CI and 2,000 ppm Fe (III)] was injected at 2.5 ml/min at room temperature.

Concentrations of Ca (II) and Fe (III) in the effluent collected from the coreflood experiment were measured by ICP. Results of the one without GLDA-NaH_3 were plotted in **Fig. 37**.

The Ca (II) concentration reached the highest point of 3,200 ppm at the begining and quickly droped to 784 ppm. After that, the Ca (II) concentration increased back to as high as 2,489 ppm. Then it started to decrease again. It is obvious, with the reaction between HCl and the limestone core plug, calcium was dissvoled into the solution. Such reaction and dissolution led to exsistence of Ca (II) in the solution.

Ca (II), obtained from the reaction between the core plug and HCl, can interact with VES to form micelles to block the core plug inside. At this point, the decreasing concentration of Ca (II) and Fe (III) was observed. However, such micelles could be flushed out with reversal injection of sufficient DI water. Then it was noted the concentration of both Ca (II) and Fe (III) increased afterwards.

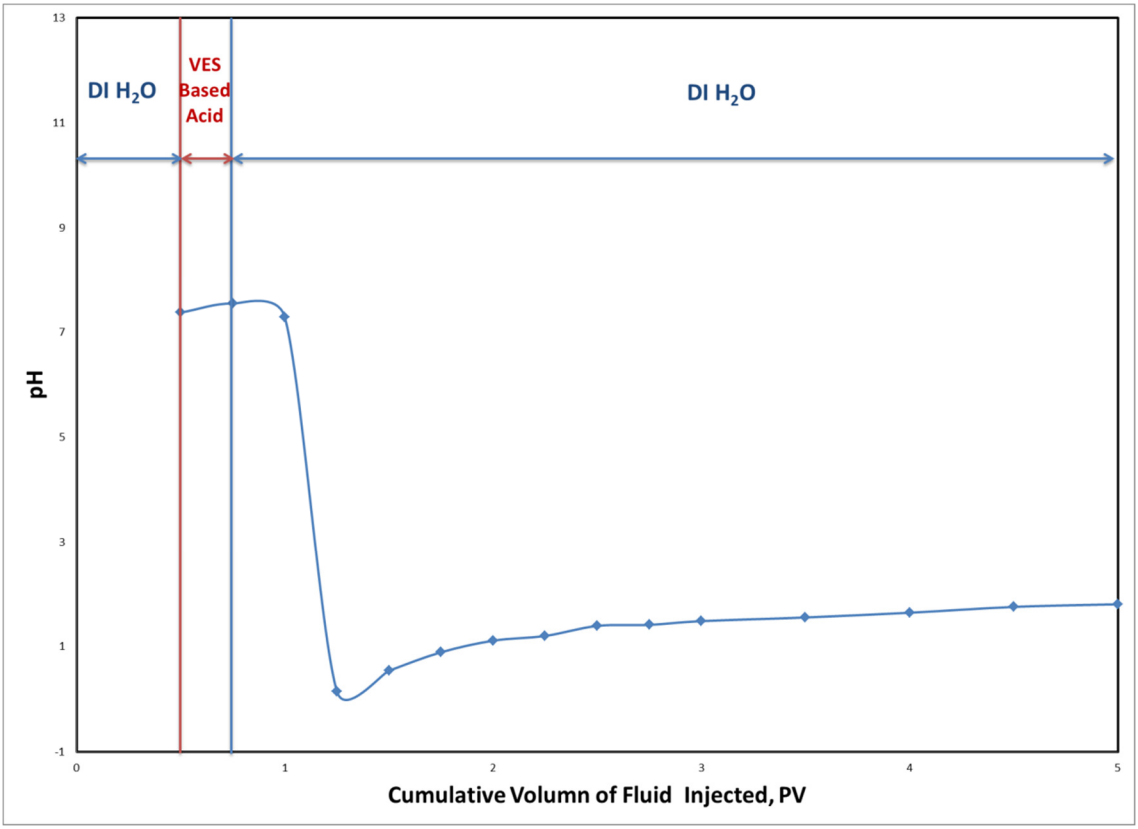

Fig. 38—pH values of the effluent from the coreflood experiment. VES-1-based acid [4 vol% VES-1, 20 wt% HCl, 0.5 vol% CI and 2,000 ppm Fe (III)] was injected at 2.5 ml/min at room temperature.

The pH of the effluents was also measured and plotted in **Fig. 38**. When the acid was not flushed out, the pH of the fluid stayed at about 7. However, when the acid came out, the solution pH was decreased to no more than 2 even after injection of 120 ml (4 times the pore volume) DI water.

Concentrations of Ca (II) and Fe (III) in the fluid collected from the coreflood experiment were measured by ICP. The results of the one with GLDA-NaH_3 [1:1 mole ratio to Fe (III)] were plotted in **Fig. 39**.

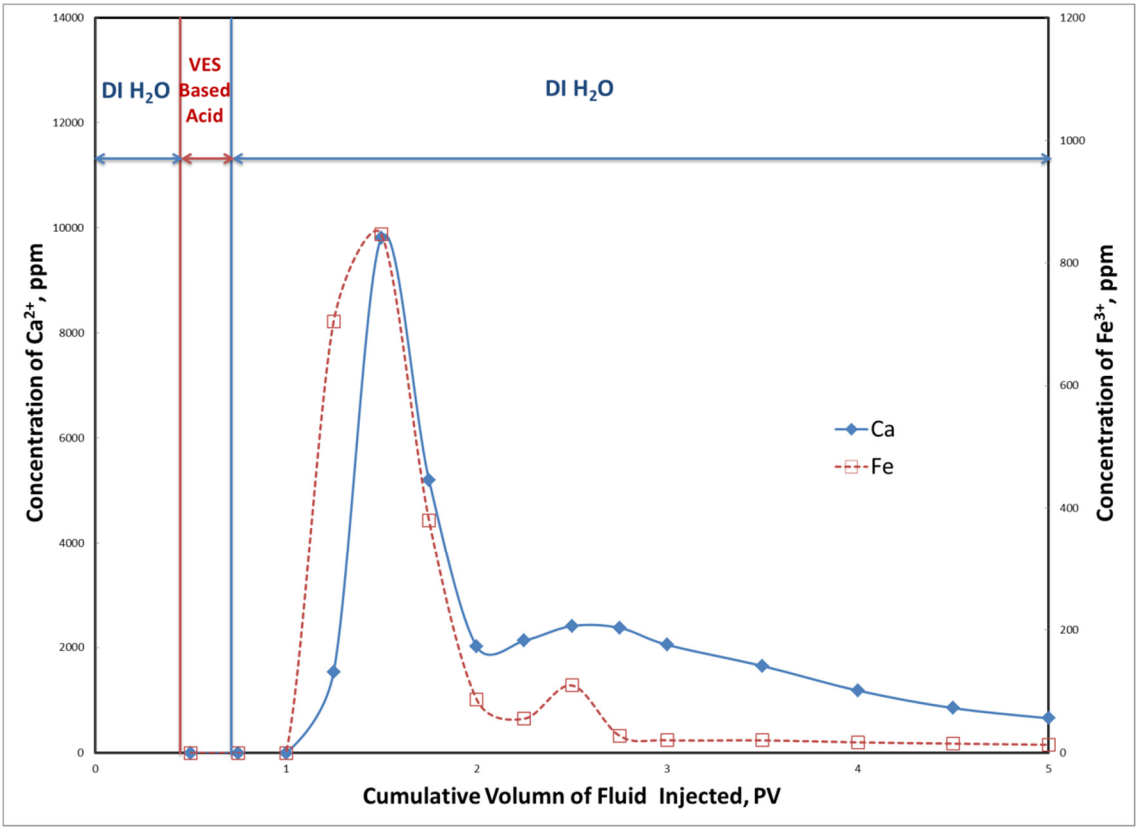

Fig. 39—Concentrations of Ca^{2+} and Fe^{3+} in effluent from the coreflood experiment. VES-1-based acid (4 vol% VES-1, 20 wt% HCl, 0.5 vol% CI, 2,000 ppm Fe (III) and GLDA-NaH_3 [1:1 mole ratio to Fe (III)]) was injected at 2.5 ml/min at room temperature.

Similar to the results of the coreflood experiment without chelating agent GLDA-NaH, Ca (II) concentration reached the highest point of 9,806 ppm at the begining and quickly droped to 2,131 ppm. After that, the Ca (II) concentration increased back to as high as 2,407 ppm. Then it started to decrease. The concentration of Fe (III) showed the same tendency: it reached the highest point at the beginning, decresed to a low point, and then increased again. Obviously, it was the formation and removal of VES micelles lead to this observation.

However, it is noticeable in the effluents from the sample with chelating agent GLDA-NaH_3, that both the concentrations of Ca (II) and Fe (III) are higher than the ones without GLDA-NaH_3. Also, as shown in **Table 3**, the total amount of Fe (III) was calculated respectively.

Table 3—Total Fe (III) Amount.

Sample Name	Fe (III) Amount (mg)
Total Injected	18.0
Without GLDA-NaH_3	8.3 (46.1%)
With GLDA-NaH_3	17.7 (98.3%)

The photo of the inlet side (side of injection of VES-based acids) of the core plugs is shown in **Fig. 40**.

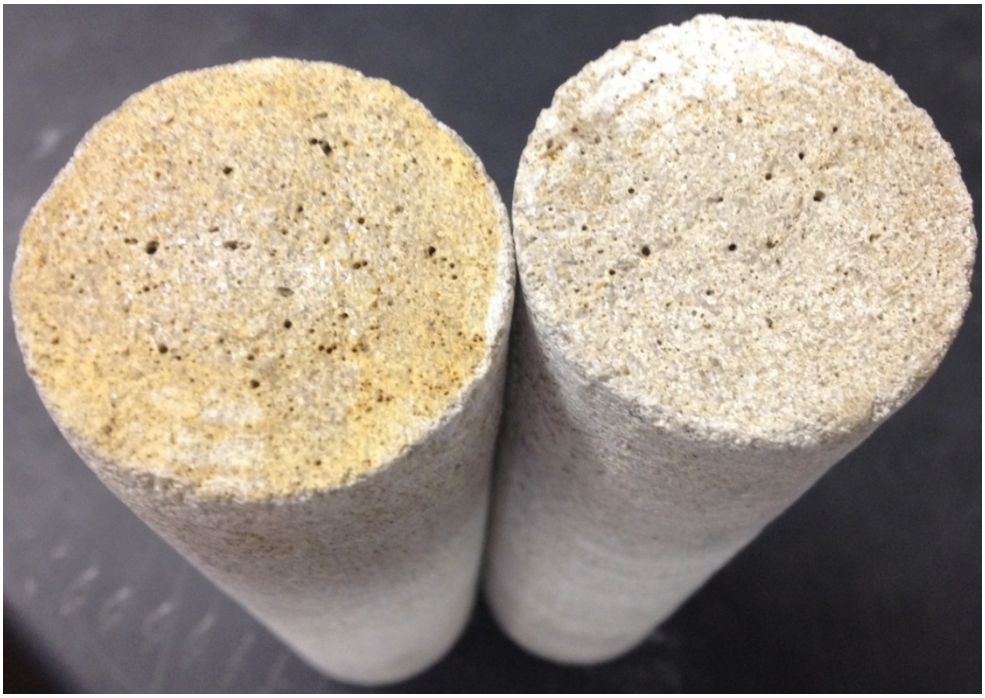

Fig. 40—Photo of inlet face of core plugs: no chelating agent was added (left) and 1:1 mole ratio GLDA-NaH_3 was added (right).

Based on the Fe (III) amount calculation and photo above, it is obvious that with the addition of GLDA-NaH_3 into the VES-1-based acid at the Fe (III) concentration of 2,000 ppm, Fe (III) was bonded to the GLDA and flushed out more easily. This observation indicated that even the apparent viscosity of the sample was not changed much, GLDA still worked on protecting the VES in solution.

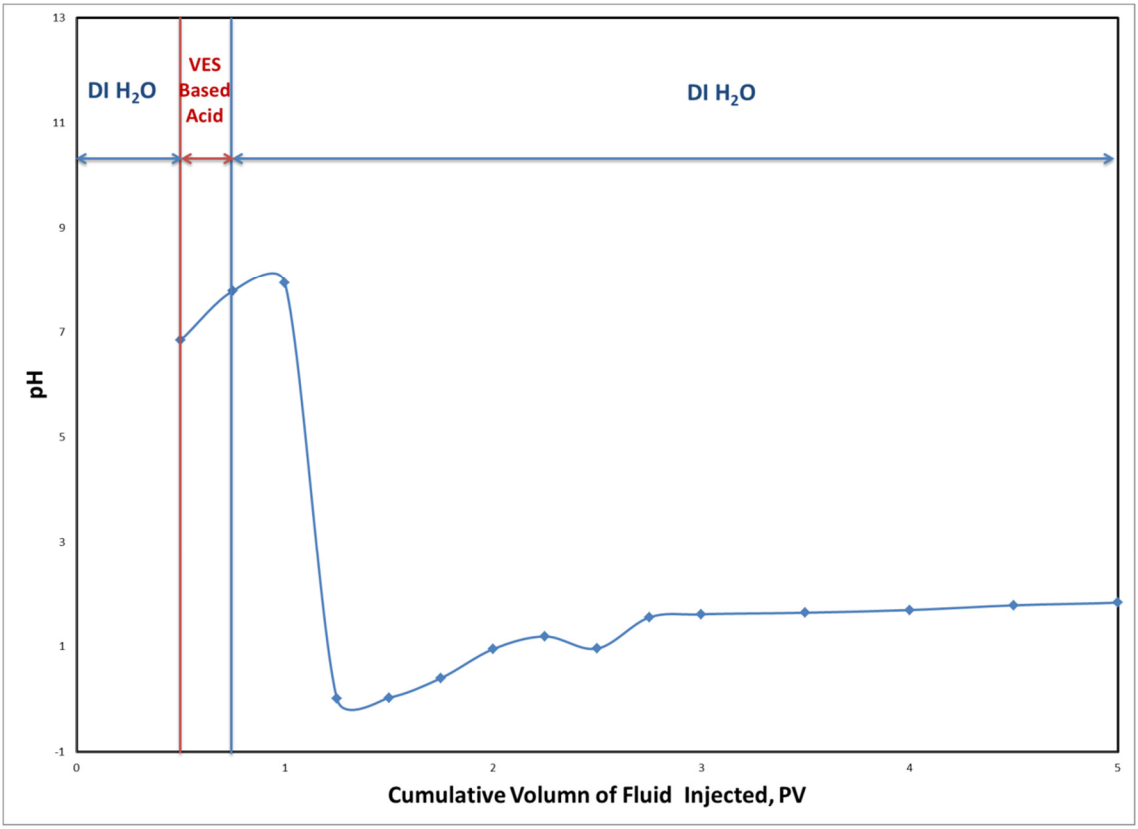

Fig. 41—pH values of effluent from the coreflood experiment. VES-1-based acid (4 vol% VES-1, 20 wt% HCl, 0.5 vol% CI, 2,000 ppm Fe (III) and GLDA-NaH_3 [1:1 mole ratio to Fe (III)]) was injected at 2.5 ml/min at room temperature.

The pH value of effluents was also measured and plotted in **Fig. 41**. Similar to the samples without adding GLDA-NaH_3, when the acid was not flushed out, the pH of the fluid stayed at about 7. However, when the acid was washed out, the solution pH decreased to less than 2 after the injection of 120 ml (4 times the pore volume) DI water.

CHAPTER V

CONCLUSIONS

Interaction between Fe (III) and two viscoelastic surfactants (VES-1 and VES-2) were studied. A method of utilizing chelating agents to protect VES was examined and results were discussed. The following conclusions could be drawn:

1. The interactions between Fe (III) and two viscoelastic surfactants (VES-1 and VES-2) were studied in 20 wt% HCl acid. The apparent viscosity of VES solutions increased at low Fe (III) concentrations and decreased at relatively higher Fe (III) concentrations because of the interaction between Fe (III) and VES. Both VES-based acids can react with Fe (III) and precipitate in high Fe (III) concentration environments. And the precipitate is a complex containing both iron and VES.

2. The formation of a negatively charged complex, $[FeCl_4]^-$, in a high concentration of HCl, leads to the interaction between Fe (III) and VES.

3. Chelating agents GLDA-NaH_3 and HEDTA-NaH_2 [1:1 mole ratio to Fe (III)] show an effective protection of VES at relatively low Fe (III) concentrations.

REFERENCES

Al-Nakhli, A.R., Nasr-El-Din, H.A., and Al-Baiyat, I.A. 2008. Interactions of Iron and Viscoelastic Surfactants: A New Formation-Damage Mechanism. Paper SPE 112465 presented at the SPE International Symposium and Exhibition on Formation Damage Control, Lafayette, Louisiana, 13-15 February.

Card, R.J., Brown, J.E., Vinod, P.S., Willberg, D.M., Samuel, M.M., and Chang, F.F. 1999. Methods for Limiting the Inflow of Formation Water and for Stimulating Subterranean Formation. US Patent No. 5,979,557.

Chang, F.F., Thomas, R.L., and Fu, D.K. 1998. A New Material and Novel Technique for Matrix Stimulation in High-Water-Cut Oil Wells. Paper SPE 39592 presented at the SPE Formation Damage Control Conference, Lafayette, Louisiana, 18-19 February.

Crews, J.B. and Huang, T. 2007. Internal Breakers for Viscoelastic-Surfactant Fracturing Fluids. Paper SPE 106216 presented at the International Symposium on Oilfield Chemistry, Houston, Texas, 28 Feburary-2 March.

Deysarkar, A.K., Dawson, J.C., Sedillo, L.P., and Knoll-Davis, S. 1984. Crosslinked Acid Gel. *J. Canadian Petroleum Technology* **23**(1): 26-32.

Dill, W. and Fredette, G. 1983. Iron Control in the Appalachian Basin. Paper SPE 12319 presented at the SPE Eastern Regional Meeting, Pittsburgh, Pennsylvania, 9-11 November.

Economides, M.J., Hill, A.D., and Ehlig-Economides, C. 1994. *Petroleum Production Systems*. Upper Saddle River, New Jersey, Prentice Hall: 392-403.

Frenier, W.W., Wilson, D., and Crump, D. 2000. Use of Highly Acid-Soluble Chelating Agents in Well Stimulation Services. Paper SPE 63242 presented at the SPE Annual Technical Conference and Exhibition, Dallas, Texas, 1-4 October.

Fu, D. and Chang, F. 2005. Compositions and Methods for Treating a Subterranean Formation. US Patent No. 6,929,070 B2.

Gamlen, G.A. and Jordan, D.O. 1953. A Spectrophotometric Study of the Iron (III) Chloro-Complexes. *J. Chem. Soc.* 1435–1443.

Gougler Jr., P.D., Hendrick, J.E., and Coulter, A.W. 1985. Field Investigation Identifies Source and Magnitude of Iron Problems. Paper SPE 13812 presented at the SPE Production Operations Symposium, Oklahoma City, Oklahoma, 10-12 March.

Hall, B.E. and Dill, W.R. 1988. Iron Control Additivies for Limestone and Sandstone Acidizing of Sweet and Sour Wells. Paper SPE 17157 presented at the SPE Formation Damage Control Symposium, Bakersfield, California, 8-9 February.

Jacobs, I.C. and Thorne, M.A. 1986. Asphaltene Precipitation During Acid Stimulation Treatments. Paper SPE 14823 presented at the Seventh SPE Symposium on Formation Damage Control, Lafayette, Louisiana, 26-27 February.

Lynn, J.D. and Nasr-El-Din, H.A. 2001. A Core-Based Comparison of the Reaction Characteristics of Emulsified and In Situ Gelled Acids in Low Permeability, High Temperature, Gas Bearing Carbonates. Paper SPE 65386 presented at the SPE International Symposium on Oilfield Chemistry, Houston, Texas, 13-16 Feburary.

Metcalf, S., Lopez, H., Hoff, C., and Woo, G. 2000. Gas Production from Low Permeability Carbonates Enhanced Through Usage of a New Acid Polymer System. Paper SPE 59756 presented at the SPE/CERI Gas Technology Symposium, Calgary, Canada, 3-5 April.

Nachtrieb. N.H. and Conway, J.G. 1948. The Extration of Ferric Chloride by Isopropyl Ether. I. *J. Am. Chem. Soc.* **70**(11): 3547-3552.

Nasr-El-Din, H.A., Taylor, K.C., and Al-Haljji, H.H. 2002. Propagation of Cross-Linkers Used in Gelled Acids in Carbonate Reserviors. Paper SPE 75257 presented at the SPE/DOE Improved Oil Recovery Symposium, Tulsa, Oklahoma, 13-17 April.

Pabley, A.S., Ewing, B.C., and Callaway, R.E. 1982. Performance of Crosslinked Hydrochloric Acid in the Rocky Mountain Region. Paper SPE 10877 presented at the SPE Rocky Mountain Regional Meeting, Billings, Montana, 19-21 May.

Rabinowitch, E. and Stockmayer, W.H. 1942. Association of Ferric Ions with Chloride, Bromide and Hydroxyl Ions (A Spectroscopic Study). *J. Am. Chem. Soc.* **64**(2): 335–347.

Rosen, M.J., Zhao, F., and Murphy, D.D. 1987. Two-Phase Mixed Indicator Method for the Determination of Zwitterionic Surfactants. *J. Am. Oil Chem.* Soc. **64**(3): 439-441.

Sharma, S.V. 1974. Ramam Study of Ferric Chloride Solutions and Hydrated Melts. *J. Chem. Phys.* **60**(4): 1368-1375.

Taylor, K.C., Nasr-El-Din, H.A., and Al-Alawi, M.J. 1999. Systematic Study of Iron Control Chemicals Used During Well Stimulation. *SPE Journal* **4**(1): 19-24.

Williams, B.B., Gidley, J.L., and Schechter, R.S., 1979. *Acidizing Fundamentals*. Monograph Series, SPE, Dallas, Texas: 1-11.

Yeager, V. and Shuchart, C. 1997. In Situ Gels Improve Formation Acidizing. *Oil & Gas J.* **95**(3): 70-72.

Yu, M., Mohamed, M.A., and Nasr-El-Din, H.A. 2009. Quantitative Analysis of Viscoelastic Surfactants. Paper SPE 121715 presented at SPE International Symposium on Oilfield Chemistry, The Woodlands, Texas, 20-22 April.

Yu, M., Mahmoud, M.A., and Nasr-El-Din, H.A. 2011. Propagation and Retention of Viscoelastic Surfactants Following Matrix-Acidizing Treatments in Carbonate Cores. *SPE Journal* **16**(4): 993-1001.